Naval Research Laboratory

Washington, DC 20375-5000

NRL Memorandum Report 6013

Excitation and Ionization Cross Sections for Electron-Beam Energy Deposition in High Temperature Air

RONALD D. TAYLOR

Berkeley Research Associates
Springfield, VA 22150

A.W. ALI

Plasma Physics Division

July 9, 1987

SECURITY CLASSIFICATION OF THIS PAGE

REPORT DOCUMENTATION PAGE

1a. REPORT SECURITY CLASSIFICATION UNCLASSIFIED	1b. RESTRICTIVE MARKINGS AD-A183074
2a. SECURITY CLASSIFICATION AUTHORITY	3. DISTRIBUTION/AVAILABILITY OF REPORT Approved for public release; distribution unlimited.
2b. DECLASSIFICATION/DOWNGRADING SCHEDULE	
4. PERFORMING ORGANIZATION REPORT NUMBER(S) NRL Memorandum Report 6013	5. MONITORING ORGANIZATION REPORT NUMBER(S)
6a. NAME OF PERFORMING ORGANIZATION Naval Research Laboratory 6b. OFFICE SYMBOL (If applicable) Code 4700.1	7a. NAME OF MONITORING ORGANIZATION
6c. ADDRESS (City, State, and ZIP Code) Washington, DC 20375-5000	7b. ADDRESS (City, State, and ZIP Code)
8a. NAME OF FUNDING/SPONSORING ORGANIZATION DARPA 8b. OFFICE SYMBOL (If applicable)	9. PROCUREMENT INSTRUMENT IDENTIFICATION NUMBER
8c. ADDRESS (City, State, and ZIP Code) Arlington, VA 22209	10. SOURCE OF FUNDING NUMBERS PROGRAM ELEMENT NO. 62707E; PROJECT NO. N60921-86-WR-W0233; TASK NO. ARPA Order 4395, A63; WORK UNIT ACCESSION NO. DN680-415

11. TITLE (Include Security Classification)
Excitation and Ionization Cross Sections for Electron-Beam Energy Deposition in High Temperature Air

12. PERSONAL AUTHOR(S)
Taylor,+ Ronald D. and Ali, A.W.

13a. TYPE OF REPORT	13b. TIME COVERED	14. DATE OF REPORT (Year, Month, Day)	15. PAGE COUNT
Interim	FROM _____ TO _____	1987 July 9	53

16. SUPPLEMENTARY NOTATION
+Berkeley Research Associates, P.O. Box 852, Springfield, VA 22150

17. COSATI CODES		
FIELD	GROUP	SUB-GROUP

18. SUBJECT TERMS (Continue on reverse if necessary and identify by block number)
Ionization cross sections, Excitation cross sections, High energy electron, Nitrogen; Oxygen.

19. ABSTRACT (Continue on reverse if necessary and identify by block number)

Electron impact excitation and ionization cross sections for N, N_ω^+, O, and O_ω^+ are provided. Electron kinetic energies range from threshold to $\geq$ 5 MeV. Available experimental and theoretical results are summarized and compared. Keywords:

20. DISTRIBUTION/AVAILABILITY OF ABSTRACT	21. ABSTRACT SECURITY CLASSIFICATION
☒ UNCLASSIFIED/UNLIMITED ☐ SAME AS RPT. ☐ DTIC USERS	UNCLASSIFIED

22a. NAME OF RESPONSIBLE INDIVIDUAL	22b. TELEPHONE (Include Area Code)	22c. OFFICE SYMBOL
A.W. Ali	(202) 767-3762	Code 4700.1

DD FORM 1473, 84 MAR 83 APR edition may be used until exhausted. All other editions are obsolete.

SECURITY CLASSIFICATION OF THIS PAGE

CONTENTS

EXCITATION AND IONIZATION CROSS SECTIONS FOR ELECTRON-BEAM ENERGY DEPOSITION IN HIGH TEMPERATURE AIR

1. INTRODUCTION

Electron beam propagation through the atmosphere is currently an area of active research. Numerical codes have been developed which, among other things, demonstrate the sensitivity of beam propagation to air chemistry. It is necessary, therefore, that chemistry codes accurately describe the relevant atomic, molecular, and radiative processes. Electron production and energy deposition are two such processes.

In general, detailed studies of energy deposition by electrons in specific gases require a complete set of cross sections for electron impact excitation and ionization of the constituent species. It is well known that the dominant constituents of heated air are atomic oxygen and nitrogen and their ions. The purpose of this report is to assemble the appropriate cross sections for O, N, O^+, and N^+ excitation and ionization for electron kinetic energies ranging from threshold to several MeV. Where possible, analytic expressions are given and compared to existing experimental results or other theoretical approaches. This information can readily be used as input for a deposition calculation of relativistic electron beams propagating through air.

Although experiments designed to measure the secondary electrons produced through impact ionization of the above species have not yet been performed, other gases have been investigated. The benchmark experiments of Opal et al.[1,2] on a number of atomic and simple molecular gases (including He, N_2, and, O_2) are worth noting. These experiments provided a detailed characterization of the doubly-differential, singly-differential and total ionization cross sections which subsequently served to guide theoretical calculations on these gases as well as others. Although recent experiments[3] on He point to some inconsistencies, these do not appear to be severe.

Green and coworkers[4-13] have been leaders in developing a theoretical base for studying electron production and energy deposition in atmospheric gases such as He, N_2, O_2, and O. In general, they have

Manuscript approved April 7, 1987

utilized the continuous slowing down approximation (CSDA) to solve the deposition problem. Peterson[14] demonstrated that while the CSDA approach suffices for high energy electrons, alternative approaches such as discrete energy loss (DEL) descriptions must be used to account for low energy electron loss. DEL approaches have been used by various groups[15-21] to investigate energy deposition in these same gases. However, modifications to the CSDA approach also prove useful.[22]

Information on experimental and theoretical collisional cross sections for O, N, O^+, and N^+ has been presented previously by Ali.[23] In this report, that information is updated, where possible, and extended to higher energy ranges. Differential cross section information is also discussed. In the absence of specific experimental cross section measurements or theoretical calculations, the efforts discussed above serve as a useful guide for obtaining such information. As expected, detailed cross section measurements and calculations for heated air do not exist for relativistic energies. In this regime, the Bethe formula[24] based on the Born approximation is of general use. Inokuti and collaborators[25,26] have presented an excellent discussion of the Bethe theory for inelastic collisions of fast charged particles with atoms.

2. ELECTRON IMPACT EXCITATION CROSS SECTIONS

2.1 Optically Allowed Transitions - Oxygen Atom

For an optically allowed transition from state i ⇒ j, the electron impact excitation cross section is given by

$$\sigma_{ij} = A_{ij} \frac{4\pi a_o^2 R^2 f_{ij}}{E^2} \left(\frac{E}{E_{ij}} - 1 \right) \left\{ \ln \left[\frac{4 C_{ij} E}{E_{ij}} (1 - \beta^2)^{-1} \right] - \beta^2 \right\} , \quad (1)$$

where πa_o^2 is the atomic unit cross section (0.88×10^{-16} cm^2), R the hydrogen atom ionization potential (13.60 eV), E_{ij} the transition energy ($E_j - E_i$), f_{ij} the optical oscillator strength, A_{ij} and C_{ij} adjustable parameters, and $\beta = v/c$ where v is the electron velocity. The energy E is $mv^2/2$ where m is the electron rest mass. E is equivalent to the electron kinetic energy provided it is less than 10^4 eV; relativistic effects begin to play a role above that value . Throughout the report cross sections are assumed equal to 0.0 for energies less than the excitation (or ionization) thresholds. In the nonrelativistic limit, Eq. (1) can be written in the form

$$\sigma_{ij} = \frac{8\pi}{\sqrt{3}} \frac{R^2}{E E_{ij}} f_{ij} g_{ij} \pi a_o^2 , \quad (2)$$

where g_{ij} is an effective Gaunt factor given by

$$g_{ij} = A_{ij} \frac{\sqrt{3}}{2\pi} \left(1 - \frac{E_{ij}}{E} \right) \ln \left[\frac{4 E}{E_{ij}} C_{ij} \right] . \quad (3)$$

Eq. (2) is a standard form for the excitation cross section subject to the Born-Bethe approximation which is valid at high energies where distant encounters are most important and short range interactions between the free and atomic electrons can be neglected. Eq. (3) is a form for the effective Gaunt factor proposed by Drawin,[27] which modifies the cross section so as to account for low energy collisions in a simple way. Finally, by incorporating the relativistic corrections, Eq. (1) gives an expression which spans the entire energy range from threshold to approximately 10^9 eV. Above that energy, it is no longer valid to neglect coupling to the radiation field.

The electron impact excitation cross sections for the $^3P \rightarrow {}^3S^o$ and $^3P \rightarrow {}^3D^o$ transitions (1304 Å and 1027 Å) are shown in Figs. 1 and 2 for electron energies up to 300 eV. These results are obtained from Eq. (1) using parameters given in Table 1. In general, the oscillator strengths for optically allowed transitions are taken from Wiese et al.,[28] however, for the 1304 Å transition f_{ij} is assumed to be 0.048. This is the generally accepted experimental value, the most recent measurement being that of Doering et al.[29] The experimental results discussed by Zipf and Erdman[30] are also shown for comparison. These are a revision of the earlier results of Stone and Zipf.[31] It is seen that the 1304 Å experimental values are 20 - 30% higher than our fit while the 1027 Å values are a factor of 2 - 3 larger. It should be noted that the experimental results include both direct and cascade contributions to excitation of the $^3S^o$ and $^3D^o$ states. The magnitude of the cascade contribution varies with energy and is difficult to estimate. Doering and Vaughan[32] have measured the absolute differential electron scattering cross section for the 1304 Å transition at an impact energy of 100 eV out to 120°. From these measurments they obtain a cascade-free integral value (also shown in Fig. 1) 30% less than the Zipf and Erdman result. Previous differential cross section measurements[33] extended out to only 20°.

Theoretical calculations of the $^3P \rightarrow {}^3S^o$ cross section have been performed using a variety of methods and approximations, including the impact parameter method,[34] close-coupling approximations,[35,36] and distorted-wave approximations.[37] The recent calculations of Rountree[36] are also shown in Fig. 1. These calculations are an improvement over the earlier Rountree and Henry[35] results, in part because of the use of improved oscillator strengths. The distorted-wave cross sections of Sawada and Ganas[37] are still lower than the Rountree results at low energies, however, the general agreement between experiment and theory is now rather good.

The $^3P \rightarrow {}^3S^o$ cross section, according to Eq. (1), is presented in Fig. 3 for electron kinetic energies up to 10^7 eV. A detailed examination shows that relativistic effects become pronounced at kinetic

energies greater than 10^4 eV. The expected relativistic rise[25] occurs at several MeV. Ganas[38] has used an independent-particle-model to calculate generalized oscillator strengths and integrated cross sections for energies up to 5 keV. These results are also shown on Fig. 3. In Eq. (1), detailed information about the generalized oscillator strength is contained within the parameter C_{ij}.

2.2 Optically Allowed Transitions - Nitrogen Atom

Very few experiments have attempted to measure electron impact excitation cross sections of atomic nitrogen. Stone and Zipf[39] measured the absolute cross sections for several dipole-allowed transitions from threshold up to 400 eV. Their estimated error was approximately 40%. As in other optical emission experiments, their cross sections include cascade contributions. Fig. 4 shows a comparison between Eq. (1) (parameters are given in Table 1) and their results for the $^4S^o \rightarrow {}^4P$ 1200 Å transition. In general, the experimental values are larger by a factor of 3.0. Spence and Burrow[40] have performed a cross-beam experiment to eliminate cascading and measure the 1200 Å and 1134 Å cross sections directly. Their results are restricted, however, to the threshold region, but do suggest smaller peak values in addition to the existence of a resonance in the 1200 Å case. For greater kinetic energies, the cross section, according to Eq. (1), resembles Fig. 3.

2.3 Optically Allowed Transitions - Oxygen Ion

For neutrals, the Born approximation assumes that the perturbing electron is described by plane waves. Positive ions, however, introduce an ion field which causes a distortion of the plane waves. At high energies, this distortion is negligible and the ion behaves like a neutral. However, at low energies it must be accounted for and Eq. (1) modified to be of use. Van Regemorter[41] and Seaton[42] deduced that the effective Gaunt factor in the semi-empirical formula given by Eq. (2) is approximately constant near threshold. Vainstein's[43] distorted-wave calculations for carbon ions and the hydrogenic results of Burgess[44]

provided justification for choosing a value of 0.2. Analogously, the nonrelativistic limit of Eq. (1) is given by Eq. (2) where g_{ij} is now defined as

$$g_{ij} = \begin{cases} 0.2 & E < 2.0\ E_{ij} \\ A_{ij}\ \frac{\sqrt{3}}{2\pi}\ \ln\left[\frac{4\ E}{E_{ij}}\ C_{ij}\right] & E > 2.0\ E_{ij} \end{cases} . \quad (4)$$

According to Eqs. (2) and (4), the cross section is peaked at threshold.[27] Relativistic corrections are included in the manner of Eq. (1).

Comparisons between Eqs. (2) and (4) and existing results are difficult. Although measurements[45,46] have been made on the $^4S^o \rightarrow {}^4P$ 834 Å transition, these are emission cross sections for radiation produced by electron impact on O_2 as opposed to direct excitation of O^+. Theoretical computations,[47] i.e. a limited multiconfiguration close-coupling calculation, have been carried out for this particular transition in the vicinity of the threshold. They suggest that the cross section rises more slowly and to a broader maximum than our analytic approximation (a peak of 5.7×10^{-17} cm^2 at E = 31.28 eV versus 9.4×10^{-17} cm^2 at threshold). This, however, is an isolated result and the attractiveness of the above analytic forms is in quantitatively describing, over a large energy range, an array of transitions for which no experimental or even theoretical results exist.

2.4 Optically Allowed Transitions - Nitrogen Ion

Electron impact excitation cross sections are computed in the manner discussed in section 2.3. Again there are no experimental results to compare with. The cross section for excitation of the $^3P \rightarrow {}^3P^o$ 672 Å transition is shown in Fig. 5 and compared to a calculation of Ganas,[48] in which he uses the Born approximation to calculate the

generalized oscillator strength and from that the cross section. The optical oscillator strength for both cases is 0.07. The effect of the constant effective Gaunt factor in the threshold regime is pronounced. For higher impact energies agreement is good.

2.5 Transitions Amongst Low-lying Metastable States - Oxygen Atom

Transitions which do not proceed according to dipole selection rules are optically forbidden. They may, however, proceed because of existing electric quadrupole moments, magnetic moments, or electron exchange effects. Cross sections for electron impact excitation of such transitions do not display the characteristic E^{-1} ln E behavior at high energies, but instead decrease more rapidly[49] (E^{-n}, where n = 1, 2, or 3). In many of their studies, Green and coworkers[4,5,8,9,11,12] have relied on the following simple form to describe excitation of forbidden transitions:

$$\sigma_{ij} = A_{ij} \frac{4\pi a_o^2 R^2}{\left(E E_{ij} \right)^a} \left[1 - \left(\frac{E_{ij}}{E} \right)^b \right]^c , \qquad (5)$$

where a, b, c, and A_{ij} are parameters and the other quantities are defined in section 2.1. Eq. (5), with the proper choice of parameters, reduces to well-known theoretical results. Collisional excitation of metastable ground states proceeds by electron exchange. When there is an accompanying change in spin multiplicity, characteristic cross sections typically peak at less than twice the threshold energy and fall off rapidly with increasing energy, i.e. E^{-3}. Drawin[27] proposed to describe both threshold and asymptotic regions with an analytic form given by Eq. (5) with (a, b, c) = (3, 2, 1). If there is no change in spin multiplicity, he proposed a form with a slower falloff and a broader peak region, i.e. (a, b, c) = (1, 1, 1). This is also the asymptotic behavior embodied in the Born-Bethe approximation.[25] Formally, information about the relativistic form factor is contained in the parameter A_{ij}.

Transitions amongst the metastable states of O include the $^3P \rightarrow {}^1D$, $^3P \rightarrow {}^1S$, and $^1D \rightarrow {}^1S$ transitions. Recent experimental studies of these transitions are limited to those of Shyn and Sharp.[50] They measured the absolute differential cross sections for the $^3P \rightarrow {}^1D$ transition at energies between 7.0 and 30.0 eV for angles between 30° and 150°. From these, the integrated cross sections were determined. First-principle calculations of these cross sections have been made by several groups.[51-53] Generally, there is good agreement between the calculations of Henry et al.[51] (threshold to 50.0 eV), Vo Ky Lan et al.[52] (0.14 to 11.0 eV), and Thomas et al.[53] (1.0 to 30.0 eV). The experiment of Shyn and Sharp, for which there is a 50% uncertainty, compares favorably with the calculations, but cannot substantiate one over another. Fig. 6 shows a comparison of the $^3P \rightarrow {}^1D$ theoretical and experimental results with an analytic fit using Eq. (5). Two sets of parameters, given in Table 2, are used. The first set was used by Green et al.[8] to give a good accounting of the threshold and peak regions. Whereas they fix these parameters over the entire energy range, which results in an E^{-1} asymptotic dependence, we modify the parameters to obtain the theoretically desired E^{-3} behavior. Ivanov and et al.[54] have used a truncated polynomial series and a similiar cutoff procedure to acheive the same results.

In Fig. 7, Eq. (5) is used to obtain excitation cross sections for the $^3P \rightarrow {}^1S$ and $^1D \rightarrow {}^1S$ transitions. For the former, two sets of parameters (see Table 2) are again used. The first set was used by Green[8] over the entire energy range, while the second set ensures an E^{-3} high-energy falloff. Together, they provide a good fit to the calculations of Henry et al.[51] The $^1D \rightarrow {}^1S$ transition is adequately modeled by a single set.

2.6 Transitions Amongst Low-lying Metastable States - Nitrogen Atom

Transitions amongst the metastable states of nitrogen are the $^4S^o \rightarrow {}^2D^o$, $^4S^o \rightarrow {}^2P^o$, and $^2D^o \rightarrow {}^2P^o$ transitions. The latest experiment to study these transitions was that of Neynaber et al.[55] In that

experiment, they measured the total cross section for electron scattering off ground state nitrogen. Detailed theoretical calculations for each of the metastable transition cross sections have been carried out by Henry et al.[51] (threshold to 50.0 eV), Ormonde et al.[56] (threshold to 20.0 eV), and Berrington et al.[57] (threshold to 35.0 eV). The theoretical results of each group predict larger total cross sections for scattering off $N(^4S^o)$ than the experiment. In addition, there is substantial discrepancy between theoretical results. Berrington et al.[57] have computed the cross sections by an R-matrix method while describing the target atom with an eight-state expansion. They have not only demonstrated convergence, but predict a resonance in the $^2D^o \rightarrow {}^2P^o$ cross section not seen by others. In general, their results are preferred.

Several theoretical results for the $^4S^o \rightarrow {}^2D^o$ transition are shown in Fig. 8 and compared to a fit given by Eq. (5). Again, two sets of parameters (see Table 2) are used to fit the low energy bahavior as well as obtain the desired E^{-3} high-energy falloff.

2.7 Transitions Amongst Low-lying Metastable States - Oxygen Ion

The transitions involving the metastable states of O^+ are the $^4S^o \rightarrow {}^2D^o$, $^4S^o \rightarrow {}^2P^o$, and $^2D^o \rightarrow {}^2P^o$ transitions. No experimental results exist for electron impact excitations of these transitions. Collision strengths for these transitions have been calculated by several groups.[51,58,59] Generally, the agreement is good. More recently, Itikawa et al.[60] have fit some of the above results to the following analytic form:

$$\sigma_{ij} = \frac{1.197 \times 10^{-15}}{g_i E} \left[\sum_{n=0}^{3} a_n \left(\frac{E_{ij}}{E} \right)^n + a_4 \ln \left(\frac{E_{ij}}{E} \right) \right] . \qquad (6)$$

In Eq. (6), g_i is the statistical weight of the initial state, a_n are parameters, and the other quantities are defined as in section 2.1. The cross section (and collision strength) is finite at threshold. Table 3 shows the parameters given in Ref. 60 for the above transitions.

2.8 Transitions Amongst Low-lying Metastable States - Nitrogen Ion

The transitions involving the N^+ metastable states are the $^3P \rightarrow {}^1D$, $^3P \rightarrow {}^1S$, and $^1D \rightarrow {}^1S$ transitions. Again, no experimental measurements have been made for these transitions as well as very few theoretical calculations. Henry et al.[51] have computed the collision strengths and are in good agreement with those calculated previously by Saraph et al.[61]

2.9 Optically Forbidden Transitions to Rydberg States - General

Electron impact excitation cross sections for optically forbidden transitions to high-lying excited states may be obtained using the general procedure developed by Green and Dutta.[5] This procedure assumes a relationship exists among states within any given Rydberg series for each ionization limit. For transitions to a specific state, excitation energies, W_{ij}, are defined by

$$W_{ij} = I_j - \frac{R}{(n - \rho)^2} \quad , \tag{7}$$

where I_j is the ionization limit, R = 13.60 eV, n is the principal quantum number for the final state outer shell electron, and ρ is the quantum defect. The constant ρ is determined by fitting the exact excitation energies, E_{ij}, to Eq. (7). For each transition, an effective oscillator strength, f_{ij}, is defined as

$$f_{ij} = \frac{f^*}{(n - \rho)^3} \quad . \tag{8}$$

In Eqs. (7 - 8), ρ and f^* vary from one Rydberg series to another, however, they remain constant within a specific series. The value of f^* is determined by equating f_{ij} with the known oscillator strength of an optically allowed transition to a state in the series. Rewritting Eq. (5), the cross section is given by

$$\sigma_{ij} = c_{ij} f_{ij} \frac{4\pi a_o^2 R^2}{W_{ij}^2} \left[1 - \left(\frac{W_{ij}}{E} \right)^b \right]^c \left(\frac{W_{ij}}{E} \right)^a \quad . \tag{9}$$

Eq. (9), with b = 1, is identical to the form used by Green and Dutta[5]. When no other experimental or theoretical results exist, the parameters c_{ij}, a, c, and ρ (again, b = 1) are chosen according to the criteria proposed by Jusick et al.[6] Assuming forms equivalent to Eq. (9), Stolarski and Green,[7] Jackman et al.,[12], and Dalgarno and Lejeune[15] present different sets of parameters for specific models of atomic oxygen. Ivanov et al.[54] give expansion parameters for a fourth-order polynomial formula similiar to an expanded version of Eq. (9). No specific results exist for N, N^+, or O^+.

2.10 Specific Optically Forbidden Transitions - Oxygen Atom

The $^3P \rightarrow {}^5S^o$ transition in atomic oxygen has been the subject of limited experimental[31] and theoretical[36,37] study. The experimental results, as presented by Stone and Zipf,[31] are 5 to 6 times larger than either the distorted wave calculations of Sawada and Ganas[37] or the close-coupling calculations of Rountree.[36] Rountree suggests that the discrepancy could be due to the uncertainty in the experimental calibration factor which, in part, depends on the (uncertain) lifetime of the $^5S^o$ state itself. The difference between theoretical results occurs mostly in the threshold and peak regions. Jackman et al.[12] have used Eq. (9) to fit the calculations of Sawada and Ganas. The experimental results are well-represented by Eq. (5). Both sets of parameters are given in Table 4, the results are shown in Fig. 9.

3. ELECTRON IMPACT IONIZATION CROSS SECTIONS

3.1 Total and Differential Cross Sections - Oxygen Atom

Both total and differential ionization cross sections are needed for electron deposition calculations. These are denoted $\sigma_i(T)$ and $\sigma_i(T,\varepsilon)$, respectively, where i indexes the state of the atom, T is the kinetic energy of the incident electron (primary) and ε the outgoing (secondary) electron. If the secondary electron is always considered to be the least energetic of the two, then the following relation holds,

$$\sigma_i(T) = \int_0^{(T-I_i)/2} \sigma_i(T,\varepsilon)\, d\varepsilon \quad , \tag{10}$$

where I_i is the ionization potential. Many different functional forms have been proposed to describe both total and differential ionization cross sections in various energy regimes. Generally, they derive from three classic results for the differential cross section, i.e. the Born-Bethe formula[25], Mott's formula[62], and Moeller's formula.[63] The Born-Bethe formula gives the cross section in the limit of high impact energies (greater than 1000 eV, but nonrelativistic) and small energy loss (and momentum transfer) by the incident electron. For high nonrelativistic impact energies and large energy transfer, Mott's formula is the appropriate approximation. When the primary electrons are relativistic, one uses Moeller's formula. In addition, results of the experiments of Opal et al.,[1,2] which were carried out for electrons with energies of 100 - 2000 eV, suggested that the cross section could be represented by a fairly simple functional form. Subsequently, others[9,11,17,19-22] have combined these results in various ways to get differential cross sections which are valid over a broader range of conditions. The total cross sections have, generally, been obtained by integrating the differential cross section approximations in a manner similiar to Eq. (10). Frequently, a functional form for $\sigma_i(T)$ is imbedded in the definition of $\sigma_i(T,\varepsilon)$; we adopt this approach below.

Finally, a useful low energy approximation (including the threshold region) for the total ionization cross sections continues to be that of Drawin.[27]

Drawing primarily from the work of Medvedev and Khokhlov,[22] $\sigma_i(T,\varepsilon)$ is given below. The index i is dropped for convenience. For the low energy regime, defined here as $T < I_i + 10$ eV,

$$\sigma(T,\varepsilon) = \frac{\sigma(T)}{\tan^{-1}\left[\frac{T-I}{2b(T)}\right]} \frac{b(T)}{b(T)^2 + \varepsilon^2} \quad . \tag{11}$$

When $T > I_i + 10$ eV then

$$\sigma(T,\varepsilon) = \frac{\sigma(T)\, b(T)}{p(T)} f(T,\varepsilon) \quad , \tag{12}$$

where

$$f(T,\varepsilon) = \frac{1}{\left(T+mc^2\right)^2} - \frac{\left(2Tmc^2+m^2c^4\right)}{\left(T+mc^2\right)^2} \frac{1}{\left(b(T)+\varepsilon\right)\left(b(T)+T-\varepsilon-I\right)}$$

$$+ \frac{1}{b(T)^2 + \left(T-\varepsilon-I\right)^2} + \frac{1}{b(T)^2 + \varepsilon^2} \quad , \tag{13}$$

and

$$p(T) = \tan^{-1}\left[\frac{T-I}{b(T)}\right] - \frac{b(T)}{T+2b(T)-I} \frac{\left(2Tmc^2+m^2c^4\right)}{\left(T+mc^2\right)^2} \ln\left[\frac{b(T)+T-I}{b(T)}\right]$$

$$+ \frac{b(T)\left(T-I\right)}{2\left(T+mc^2\right)^2} \quad . \tag{14}$$

In Eqs. (11 - 14), b(T) is a parameter, either energy dependent or constant, chosen to best fit any available data and mc^2 is the electron rest mass energy (.511 MeV).

The total ionization cross section is given, analogous to Eq. (1), by

$$\sigma_i = A_i \frac{4\pi a_o^2 R^2}{E^2} \left(\frac{E}{I_i} - 1 \right) \left\{ \ln \left[\frac{4 C_i E}{I_i} (1 - \beta^2)^{-1} \right] - \beta^2 \right\} \quad , \quad (15)$$

where $E = mv^2/2$. Again, A_i and C_i are adjustable parameters. In the nonrelativistic limit, $T \approx E$ and Eq. (15) reduces identically to the Drawin formula.[27] To obtain the Drawin formula, the parameters are defined as $A_i = 0.665\xi_i$ and $C_i = 0.3125\{1+[(Z_{eff}-1)/(Z_{eff}+2)]\}$ where ξ_i denotes the number of equivalent electrons in the i-th state and Z_{eff} the effective charge number of the nucleus acting on the electrons in the i-th state. Numerical values of ξ_i have been tabulated[27] for ionization from the ground state, specifically, ξ_i = [3.0, 3.0, 2.7, 2.5] for [N, O, N^+, O^+]. For ionization of excited states it is recommended that $\xi_i = 1.0$. These definitions provide a means for choosing A_i and C_i in the absence of experimental data or dependable theoretical calculations. For high energy electrons, Eq. (15) displays the desired E^{-1} ln E dependence and, at relativistic energies, the expected relativistic rise. For impact energies between threshold and 10^4 eV, Lotz[64] fit the E^{-1} ln E form to available experimental data (up to 1967) on cross sections for ionization of atoms and ions from the ground state, including N, N^+, O, and O^+. For numerous atomic and molecular gases, none of which are considered in this study, Rieke and Prepejchal[65] measured the ionization cross sections for electrons of kinetic energies of 0.1 - 2.7 MeV and found that the asymptotic limit of Eq. (15) suitably described those measurements.

While no experimental results exist, calculations of energy differential cross sections for electron impact of O are limited to the independent-particle-model results of Kazaks et al.[10] and Burnett and Rountree's[66] ab initio results. Eqs. (11 - 15) are scaled to the latter results, which provide a better treatment near the ionization threshold, and used to obtain the partial single differential cross sections for a 500 eV electron ionizing $O(^3P)$ (shown in Fig. 10). Ionization to the

$^4S^o$, $^2D^o$, and $^2P^o$ continua, respectively, is described using the scaling parameters given in Table 5. Representative differential ionization cross sections for higher energy primaries are shown in Fig. 11. The increase in $\sigma_i(T,\varepsilon)$ for small ε when T goes from 1 MeV to 10 MeV is a consequence of the total ionization cross section rising because of relativistic effects.

The total electron impact ionization cross section for atomic oxygen has been investigated both experimentally[67-70] and theoretically.[10,13,15,54,71-74] The cross section for ionization of $O(^3P)$, partitioned into the various channels according to Eq. (15) and the above parameters, is shown in Fig. 12. The results of Burnett and Rountree are also given. Previously,[23] decomposition of the total ionization into specific channels was accomplished using data from Dalgarno and Lejeune.[15] The two results are in close agreement for electron energies greater than 75.0 eV, however, differences of 1.0% - 3.0% exist for energies less than 75.0 eV. In Fig. 13, the total ionization cross section is given for energies up to 10 MeV. The experimental results of Brook et al.[70] are shown for comparison. A detailed illustration of the differences between existing experimental and theoretical ionization cross sections is presented in Fig. 5 of Ref. 70.

3.2 Total and Differential Cross Sections - Nitrogen Atom

To date, no experimental or theoretical results have been presented for differential ionization cross sections of atomic nitrogen. Total electron impact ionization cross sections, however, have been measured experimentally[70,75,76] and calculated theoretically.[71-74] There is good agreement between the measurements of Brook et al.[70] and those of Smith et al.[75] for energies less than 600 eV. Above that energy, Smith's results show an anomolous increase in the cross section. The measurements of Peterson[76] exceed the others by more than 100%. All of the theoretical calculations exceed the experimental data by 30% or more for energies between 30 ev and 150 eV. The theoretical results of

McGuire[73] provide the best agreement, particularly for energies greater than 200 eV. Again, a detailed illustration of the differences between existing experimental and theoretical ionization cross sections is presented in Fig. 6 of Ref. 70. In Fig. 14, the total ionization cross section according to Eq. (15) is given. We have assumed that the single ionization channel is $e + N(^4S^o) \rightarrow e + e + N^+(^3P)$, i.e. transitions to $N^+(^1D)$ and $N^+(^1S)$ are neglected since they do not occur in photoionization and, therefore, are expected to have small collision cross sections. The scaling parameters are given in Table 5. The experimental results of Brook et al. and the calculations of McGuire are shown for comparison. Since Eq. (15) does not provide a very good representation of the low energy behavior, a better appoximation for code input would be to use the experimental data for energies less than 100 eV and the analytic results for greater energies.

Eqs. (11 - 15) are again used to compute differential cross sections, but b(T) is chosen arbitrarily. Fig. 15 shows $\sigma_i(T,\varepsilon)$ for T = 0.1, 1.0, and 10.0 MeV, assuming b(T) = 15.0. The behavior is identical to that discussed above for oxygen.

3.3 Total and Differential Cross Sections - Oxygen Ion

The total ionization cross section for electron impact on O^+ has been measured experimentally[77-80] and calculated theoretically.[13,81-84] Reasonable agreement exists between the experiments. Together, these data span electron impact energies from threshold up to 10 keV. From threshold to 1 keV, the calculations of McGuire[84] and Moores[81] agree with each other and are 10 - 15% higher at the peak than the experimental results of Aitken et al.[77] The measurements of Donets and Ovsyannikov[80] exceed the corresponding classical binary-encounter-approximation calculations of Salop[82] by as much as 25% for energies of 1 - 10 keV. The ionization cross section, according to Eq. (15) with parameters given in Table 5, is presented in Fig. 16 along with the experimental results of Aitken et al.[77] and Donets et al.[80] Only ionization of $O^+(^4S^o)$ is considered. Aitken has suggested that ionization of the metastable states, $O^+(^2D^o)$ and $O^+(^2P^o)$, contributes at most 10% to the total cross section.

Ganas and Green[13] have used an independent-particle-model to calculate continuum generalized oscillator strengths from which they obtain differential cross sections. Fig. 17 shows a comparison between their results and Eqs. (11 - 15), assuming b(T) = 20.0, for primary electron energies of 500, 1000, and 5000 eV. The agreement is good.

3.4 Total and Differential Cross Sections - Nitrogen Ion

N^+ total ionization cross sections have also been measured experimentally[80,85,86] and calculated theoretically.[81-84,87,88] Good agreement exists between the measurements of Hasted et al.[86] and Harrison et al.[85] from threshold to 500 eV. The data of Donets et al.[80] extends this region up to 7 keV. The calculations of McGuire[84] agree closely with those of Moores[81] and McCarthy et al.[88] and are within 20% of Harrison's[85] experimental results. Donets' higher energy data vary rapidly, however, exceeding these calculations by 10 - 100%. In Fig. 18, the ionization cross section, according to Eq. (15), is given and compared to the data of Harrison et al. and Donets et al. The cross section matches closely that calculated by McGuire. The parameters are $A_i = 2.0$ and $C_i = 0.39$.

ACKNOWLEDGEMENT

This work was supported by the Defense Advanced Research Projects Agency under ARPA Order No. 4395, Amendment No. 63, and monitored by the Naval Surface Weapons Center.

REFERENCES

1. C.B. Opal, W.K. Peterson, and E.C. Beaty, J. Chem. Phys. 55, 4100 (1971).

2. C.B. Opal, E.C. Beaty, and W.K. Peterson, At. Data 4, 209 (1972).

3. R.R. Goruganthu and R.A. Bonham, Phys. Rev. A34, 103 (1986).

4. L.R. Peterson, S.S. Prasad, and A.E.S. Green, Can. J. Chem. 47, 1774 (1969).

5. A.E.S. Green and S.K. Dutta, J. Geophys. Res. 72, 3933 (1967).

6. A.T. Jusick, C.E. Watson, L.R. Peterson, and A.E.S. Green, J. Geophys. Res. 72, 3943 (1967).

7. R.S. Stolarski and A.E.S. Green, J. Geophys. Res. 72, 3967 (1967).

8. A.E.S. Green and R.S. Stolarski, J. Atmos. Terr. Phys. 34, 1703 (1972).

9. A.E.S. Green and T. Sawada, J. Atmos. Terr. Phys. 34, 1719 (1972).

10. P.A. Kazaks, P.S. Ganas, and A.E.S. Green, Phys. Rev. A6, 2169 (1972).

11. H.S. Porter, C.H. Jackman, and A.E.S. Green, J. Chem. Phys. 65, 154 (1976).

12. C.H. Jackman, R.H. Garvey, and A.E.S. Green, J. Geophys. Res. 82, 5081 (1977).

13. P.S. Ganas and A.E.S. Green, J. Quant. Spectrosc. Radiat. Transfer 25, 265 (1981).

14. L. Peterson, Phys. Rev. 187, 105 (1969).

15. A. Dalgarno and G. Lejeune, Planet. Space Sci. 19, 1653 (1971).

16. S.P. Khare, J. Phys. B3, 971 (1970).

17. S.P. Khare and A. Kumar Jr, J. Phys. B10, 2239 (1977).

18. S.P. Khare and A. Kumar Jr, J. Phys. B11, 2403 (1978).

19. D.J. Strickland, D.L. Book, T.P. Coffey, and J.A. Fedder, J. Geophys. Res. 81, 2755 (1976).

20. D.J. Strickland and A.W. Ali, "A Code for the Secondary Electron Energy Distribution in Air and Some Applications", NRL Memorandum Report 4956, Washington, D.C. (1982). ADA121564

21. S. Slinker and A.W. Ali, Proceedings of the SDIO/DARPA Annual Propagation Review, Alburquerque, New Mexico (1986). Also, "Electron Energy Deposition in Atomic Oxygen", NRL Memorandum Report 5909, Washington, D.C. (1987). ADA177218

22. Y.A. Medvedev and V.D. Khokhlov, Sov. Phys. Tech. Phys. 24, 181 (1979); ibid 185 (1979).

23. A.W. Ali, "Excitation and Ionization Cross Sections for Electron Beam and Microwave Energy Deposition in Air", NRL Memorandum Report 4598, Washington, D.C. (1981). ADA103106 Also, "Electron Impact Rate Coefficients for the Low-Lying Metastable States of O, O^+, N and N^+", NRL Memorandum Report 3371, Washington, D.C. (1976). ADA031221

24. H. Bethe, Z. Physik 76, 293 (1932).

25. M. Inokuti, Rev. Mod. Phys. 43, 297 (1971).

26. M. Inokuti, Y. Itikawa, and J. Turner, Rev. Mod. Phys. 50, 23 (1978).

27. H.W. Drawin, "Collision and Transport Cross Sections", Report EUR-CEA-FC-383, Fontenay-aux-Roses (1966) and revised (1967).

28. W.L. Wiese, M.W. Smith, and B.M. Glennon, "Atomic Transition Probabilities", NSRDS-NBS4, vol. 1, U.S. Government Printing Office, Washington, D.C. (1966).

29. J.P. Doering, E.E. Gulcicek, and S.O. Vaughan, J. Geophys. Res. 90, 5279 (1985).

30. E.C. Zipf and P.W. Erdman, J. Geophys. Res. 90, 11087 (1985).

31. E.J. Stone and E.C. Zipf, J. Chem. Phys. 60, 4237 (1974).

32. J.P. Doering and S.O. Vaughan, J. Geophys. Res. 91, 3279 (1986).

33. M.A. Khakoo, W.R. Newell, and A.C.H. Smith, J. Phys. B13, 4263 (1980).

34. A.D. Stauffer and M.R.C. McDowell, Proc. Phys. Soc. 89, 289 (1966).

35. S.P. Rountree and R.J.W. Henry, Phys. Rev. A6, 2106 (1972).

36. S.P. Rountree, J. Phys. B10, 2719 (1977).

37. T. Sawada and P.S. Ganas, Phys. Rev. A7, 617 (1973).

38. P.S. Ganas, Phys. Lett. 84A, 115 (1981).

39. E.J. Stone and E.C. Zipf, J. Chem. Phys. 58, 4278 (1973).

40. D. Spence and P.D. Burrows, J. Phys. B13, 2809 (1980).

41. H. Van Regermorter, Astrophys. J. 136, 906 (1962).

42. M.J. Seaton, in Atomic and Molecular Processes (Edited by D.R. Bates) Academic Press, New York (1962).

43. L.A. Vainstein, Opt. Spectrosc. 14, 163 (1961).

44. A. Burgess, Mem. Soc. Roy. Liege 4, 299 (1961).

45. H.D. Morgan and J.E. Mentall, J. Chem. Phys. 78, 1747 (1983).

46. J.F.M. Aarts and F.J. DeHeer, Physica (Utrecht) 56, 294 (1971).

47. S. Ormande, K. Smith, B. Torres, and A.R. Davies, Phys. Rev. A8, 262 (1973).

48. P.S. Ganas, J. Chem. Phys. 72, 2197 (1980).

49. N.F. Mott and H.S.W. Massey, The Theory of Atomic Collisions (3rd edition) Clarendon Press, Oxford (1965).

50. T.W. Shyn and W.E. Sharp, J. Geophys. Res. 91, 1691 (1986).

51. R.J.W. Henry, P.G. Burke, and A.-L. Sinfailam, Phys. Rev. 178, 218 (1969).

52. Vo Ky Lan, N. Feautrier, M. Le Dourneuf, and H. Van Regemorter, J. Phys. B5, 1506 (1972).

53. L.D. Thomas and R.K. Nesbet, Phys. Rev. A11, 170 (1975).

54. V. Ye. Ivanov, N.K. Osipov, and V.A. Shneyder, Geomag. Aeron. 17, 319 (1977).

55. R.H. Neynaber, L.L. Marino, E.W. Rothe, and S.M. Trujillo, Phys. Rev. 129, 2069, (1963).

56. S. Ormonde, K. Smith, B.W. Torres, and A.R. Davies, Phys. Rev. A8, 262 (1973).

57. K.A. Berrington, P.G. Burke, and W.D. Robb, J. Phys. B8, 2500 (1975).

58. S.J. Czyzak, T.K. Krueger, P. de A.P. Martins, H.E. Saraph, and M.J. Seaton, Mon. Not. R. Astr. Soc. 148, 361 (1970).

59. A.K. Pradhan, J. Phys. B9, 433 (1976).

60. Y. Itikawa, S. Hara, T.Kato, S. Nakazaki, M.S. Pindzola, and D.H. Crandall, At. Data and Nucl. Data Tables 33, 149 (1985).

61. H.E. Saraph, M.J. Seaton, and J. Shemming, Proc. Phys. Soc. 89, 27 (1966).

62. N.F. Mott, Proc. Phys. Soc. Roy. Soc. (London) A126, 259 (1930).

63. C. Moeller, Ann. Phys. 14, 531 (1932).

64. W. Lotz, Astrophys. J. Suppl. 14, 207 (1967).

65. F.F. Rieke and W. Prepejchal, Phys. Rev. A6, 1507 (1972).

66. T. Burnett and S.P. Rountree,Phys. Rev. A20, 1468 (1979).

67. W.L. Fite and R.T. Brackman, Phys. Rev. 113, 815 (1959).

68. A. Boksenberg, Ph.D. Thesis, University of London (1961).

69. E.W. Rothe, L.L. Marino, R.H. Neynaber, and S.M. Trujillo, Phys. Rev. 125, 582 (1961).

70. E. Brook, M.F. Harrison, and A.C.H. Smith, J. Phys. B11, 3115 (1978).

71. M.J. Seaton, Phys. Rev. 113, 814 (1959).

72. G. Peach, J. Phys. B3, 328 (1970).

73. E.J. McGuire, Phys. Rev. A3, 267 (1971).

74. K. Omidvar, H.L. Kyle, and E.C. Sullivan, Phys. Rev. A5, 1174 (1972).

75. A.C.H. Smith, E. Caplinger, R.H. Neynaber, E.W. Rothe, and S.M. Trujillo, Phys. Rev. 127, 1647 (1962).

76. J.R. Peterson, in Atomic Collision Processes (Edited by M.R.C. McDowell) North-Holland, Amsterdam (1964).

77. K.L. Aitken and M.F. Harrison, J. Phys. B4, 1176 (1971).

78. M. Hamdan, K. Birkinshaw, and J.B. Hasted, J. Phys. B11, 331 (1978).

79. A. Muller, E. Salzborn, R. Frodl, R. Becker, H. Klein, and H. Winter, J. Phys. B13, 1877 (1980).

80. E.D. Donets and V.P. Ovsyannikov, Sov. Phys. JETP 53, 466 (1981).

81. D.L. Moores, J. Phys. B5, 286 (1972).

82. A. Salop, Phys. Rev. A14, 2095 (1976).

83. A. Kumar and B.N. Roy, Phys. Lett. 66A, 362 (1978).

84. E.J. McGuire, Phys. Rev. A25, 192 (1982).

85. M.F.A. Harrison, K.T. Dolder, and P.C. Thonemann, Proc. Phys. Soc. 82, 368 (1963).

86. J.B. Hasted and G.L. Awad, J. Phys. B5, 1719 (1972).

87. B.K. Thomas and J.D. Garcia, Phys. Rev. 179, 94 (1969).

88. I.E. McCarthy and A.T. Stelbovics, Phys. Rev. A28, 1322 (1983).

Table 1

Electron Impact Excitation Cross Section Parameters
for Optically Allowed Transitions

Transition	A_{ij}	C_{ij}	f_{ij}
$O(^3P) \rightarrow O(^3S^o)$	1.0	0.3125	0.048
$O(^3P) \rightarrow O(^3D^o)$	1.0	0.3125	0.010
$N(^4S^o) \rightarrow N(^4P)$	1.0	0.3125	0.130

Table 2

Electron Impact Excitation Cross Section Parameters
for Transitions Amongst N and O Metastable States

Transition	A_{ij}	a	b	c	
$O(^3P) \rightarrow O(^1D)$	0.01 97.0	1 3	1	2	$\leq$ 50.0 eV $\geq$ 50.0 eV
$O(^3P) \rightarrow O(^1S)$	0.0042 117.23	1 3	0.5	1	$\leq$ 40.0 eV $\geq$ 40.0 eV
$O(^3P) \rightarrow O(^1D)$	0.003	1	1	1	
$N(^4S^o) \rightarrow N(^2D^o)$	0.025 227.72	1 3	1	1	$\leq$ 40.0 eV $\geq$ 40.0 eV
$N(^4S^o) \rightarrow N(^2P^o)$	0.0175 356.04	1 3	1	1	$\leq$ 40.0 eV $\geq$ 40.0 eV

Table 3

Electron Impact Excitation Cross Section Parameters
for Transitions Amongst O^+ Metastable States

Transition	a_0	a_1	a_2	a_3	a_4
$O^+(^4S^o) \rightarrow O^+(^2D^o)$	2.016	-1.65	0.864	0.079	0.0
$O^+(^4S^o) \rightarrow O^+(^2P^o)$	0.231	0.316	-0.071	0.0	0.313
$O^+(^2D^o) \rightarrow O^+(^2P^o)$	3.072	-4.123	5.151	-2.322	0.0

Table 4

Electron Impact Excitation Cross Section Parameters
for $O(^3P) \rightarrow O(^5S^o)$ Transition

Eq. (9)	W_{ij}	c_{ij}	f_{ij}	a	b	c
Fit to theory	10.6	1.0	0.013	2.69	19.20	10.50

Eq. (5)	A_{ij}	a	b	c
Fit to experiment	5880.0	3	1	2

Table 5

Electron Impact Ionization Cross Section Parameters

Channel	A_i	C_i	b(T)
$O(^3P) \rightarrow O^+(^4S^o)$	0.65	0.25	13.0
$O(^3P) \rightarrow O^+(^2D^o)$	1.0	0.25	17.0
$O(^3P) \rightarrow O^+(^2P^o)$	0.55	0.25	19.0
$N(^4S^o) \rightarrow N^+(^3P)$	2.20	0.25	15.0
$O^+(^4S^o) \rightarrow O^{++}(^3P)$	2.70	0.25	20.0
$N^+(^3P) \rightarrow N^{++}(^2P^o)$	2.0	0.25	--

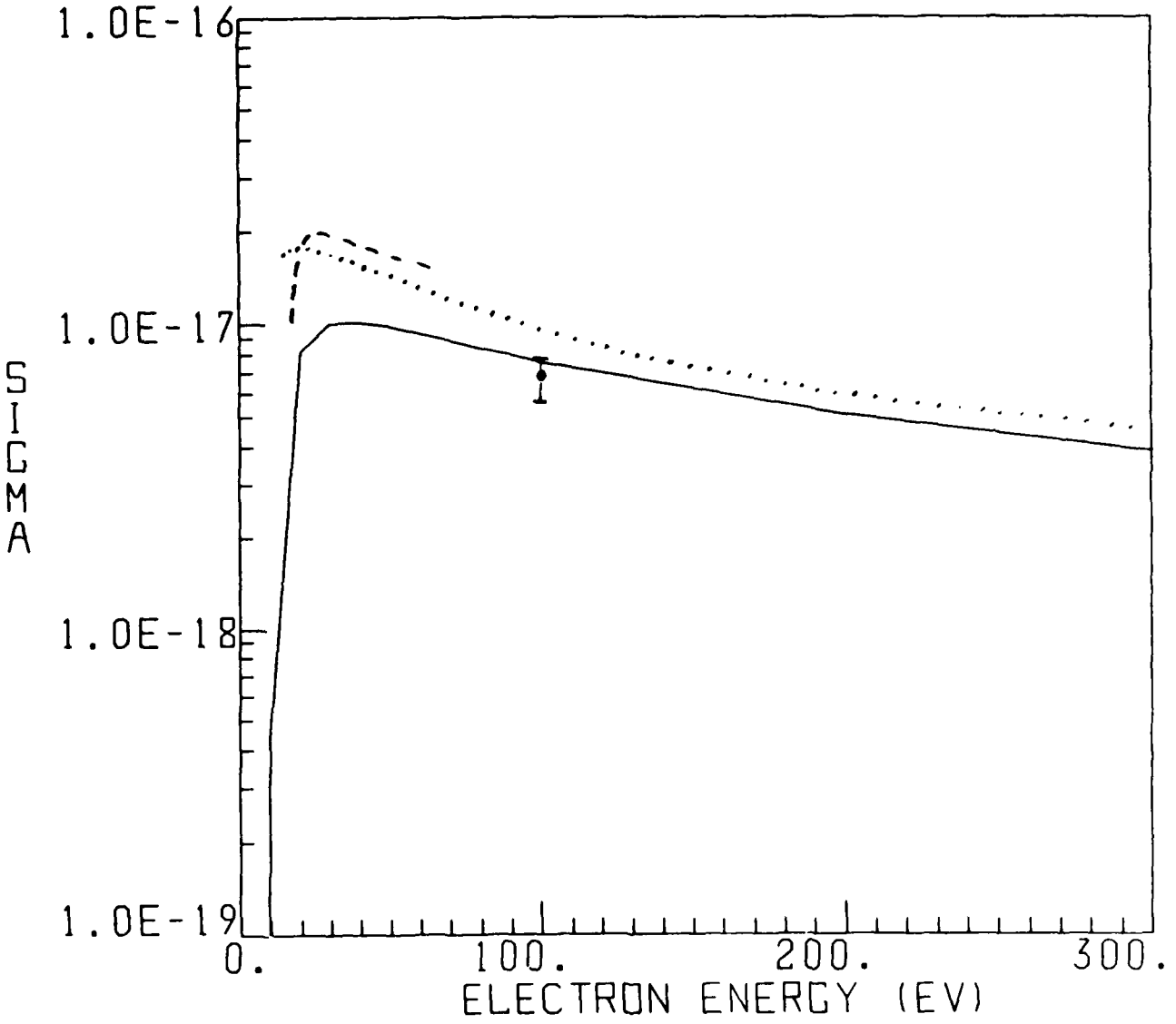

Fig. 1. Electron impact excitation cross sections for $O(^3P \rightarrow {}^3S^o)$ 1304 Å transition (solid line - Eq. (1), dotted line - Ref. 30, dashed line - Ref. 36, and solid circle - Ref. 32).

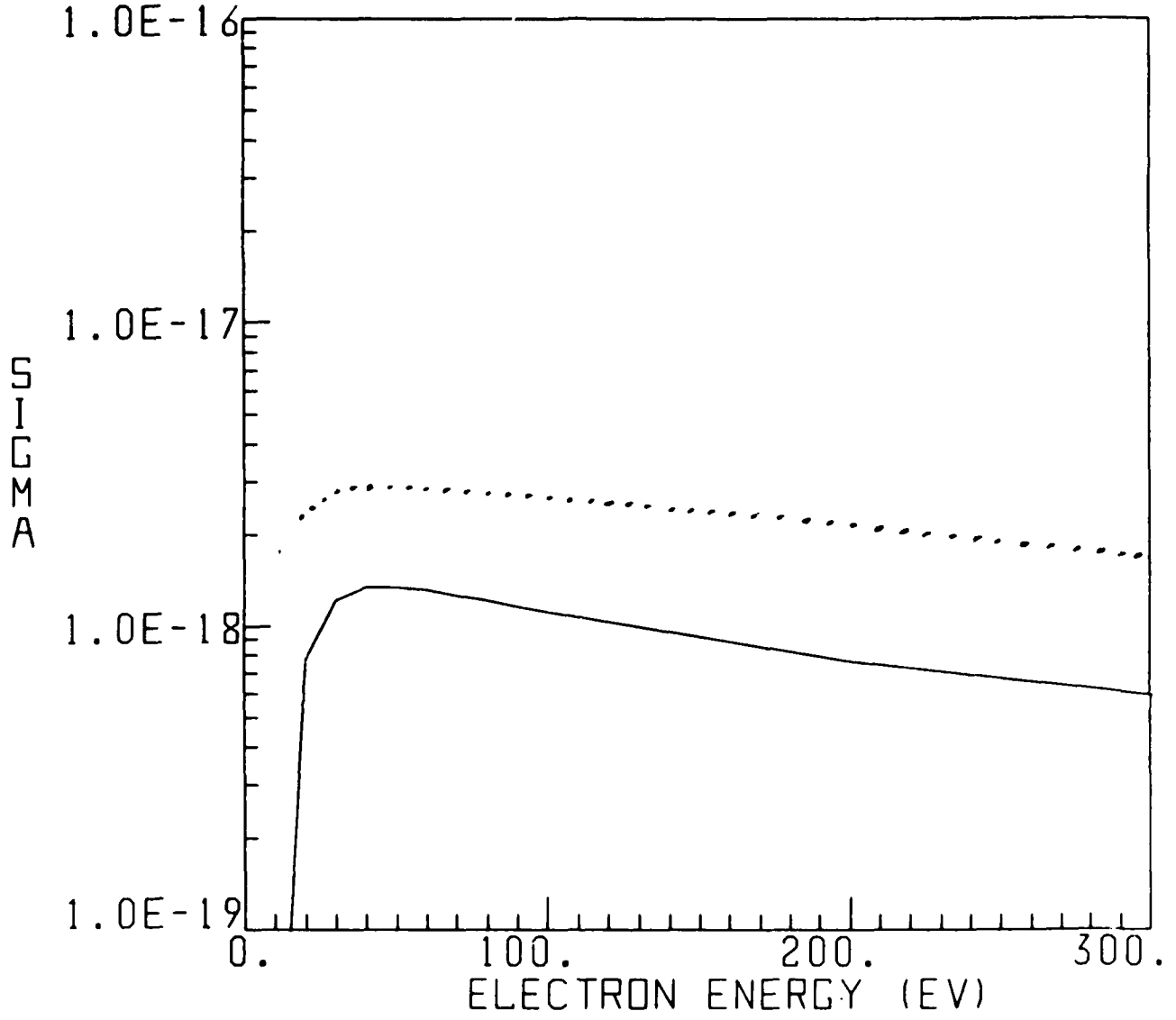

Fig. 2. Electron impact excitation cross sections for O($^3P \rightarrow {}^3D^o$) 1027 Å transition (solid line - Eq. (1) and dotted line - Ref. 30).

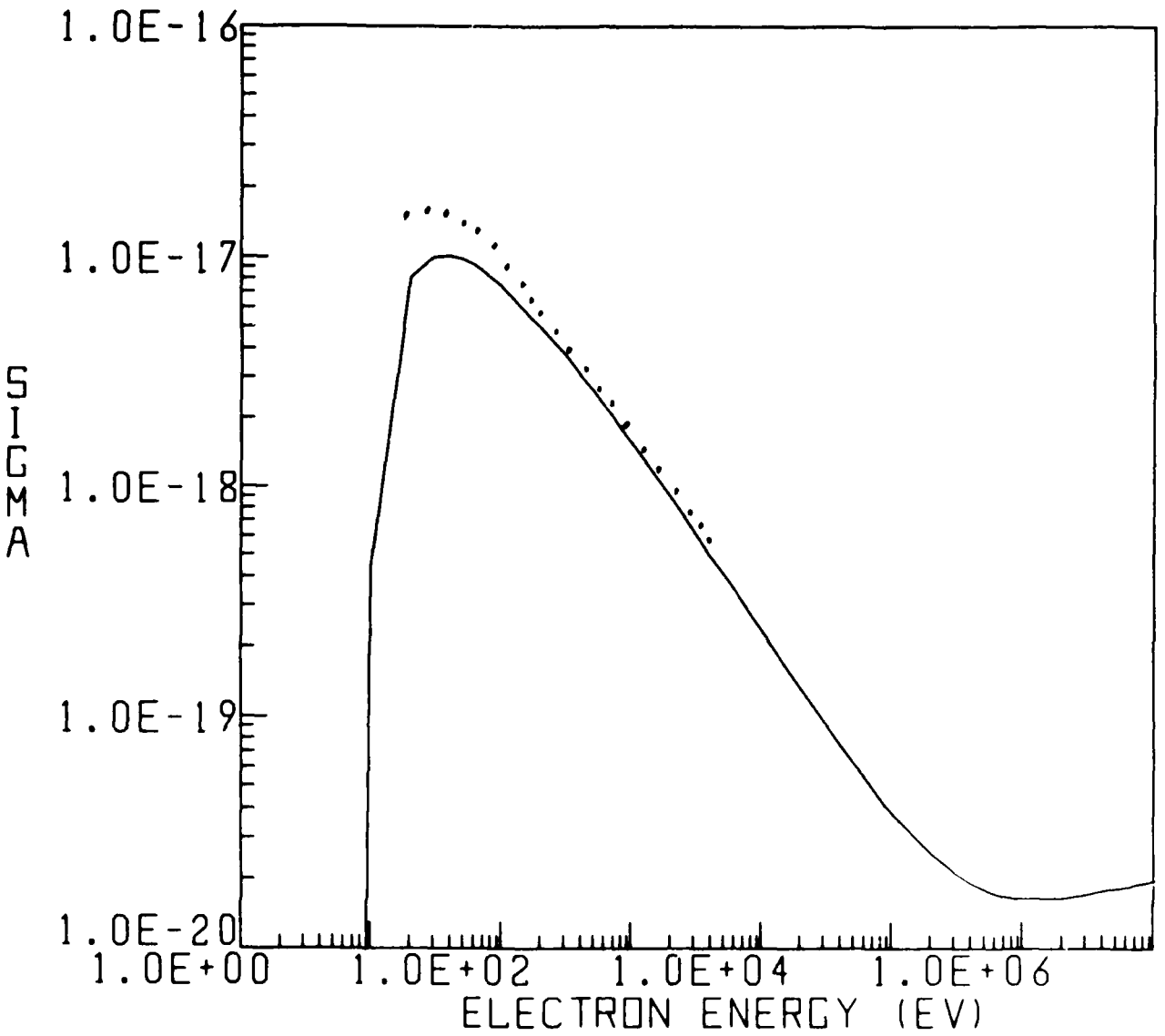

Fig. 3. Electron impact excitation cross sections for $O(^3P \rightarrow {}^3S^o)$ 1304 Å transition (solid line - Eq. (1), dotted line - Ref. 38).

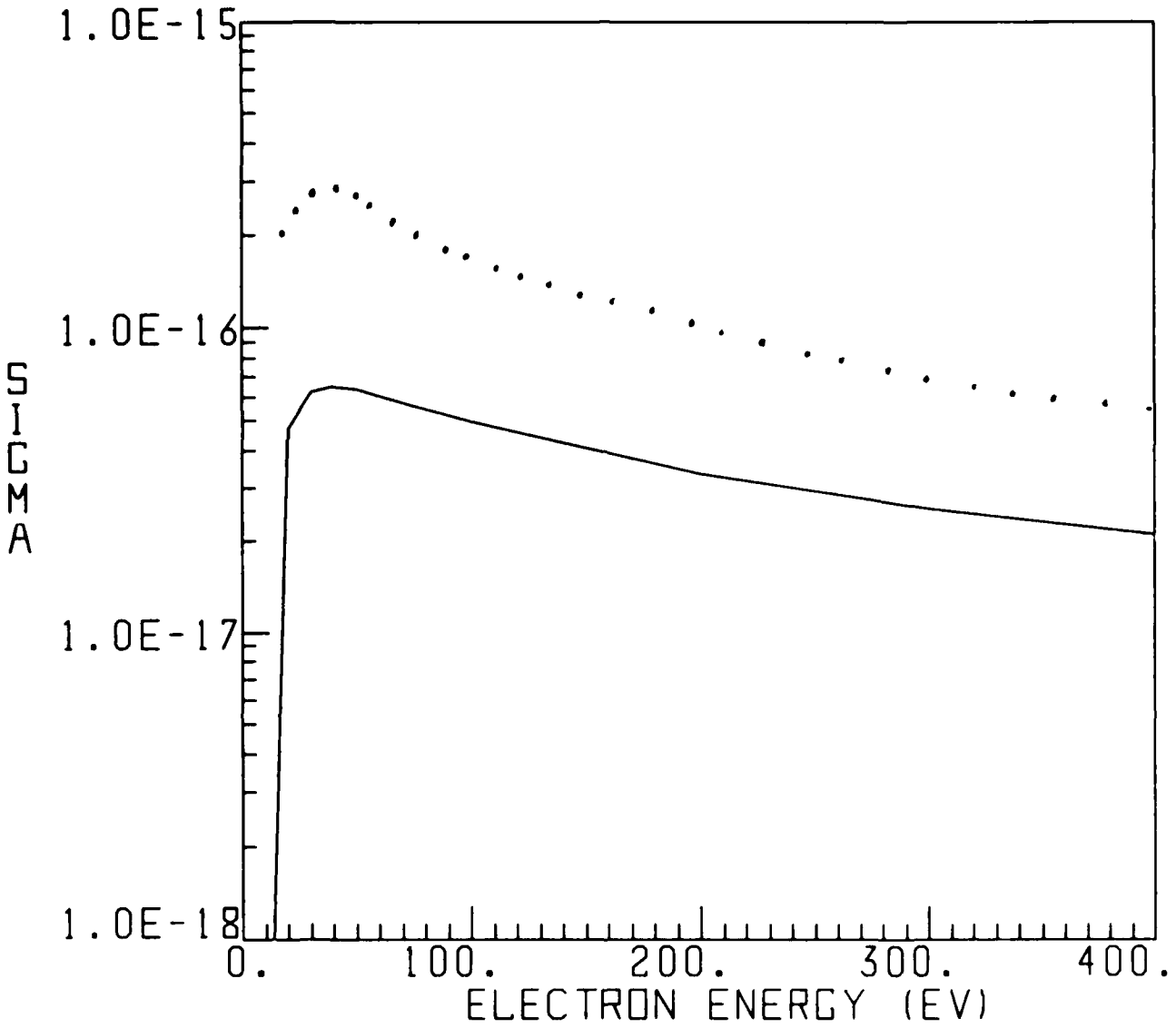

Fig. 4. Electron impact excitation cross sections for $N(^4S^o \rightarrow {}^4P)$ 1200 Å transition (solid line - Eq. (1), dotted line - Ref. 39).

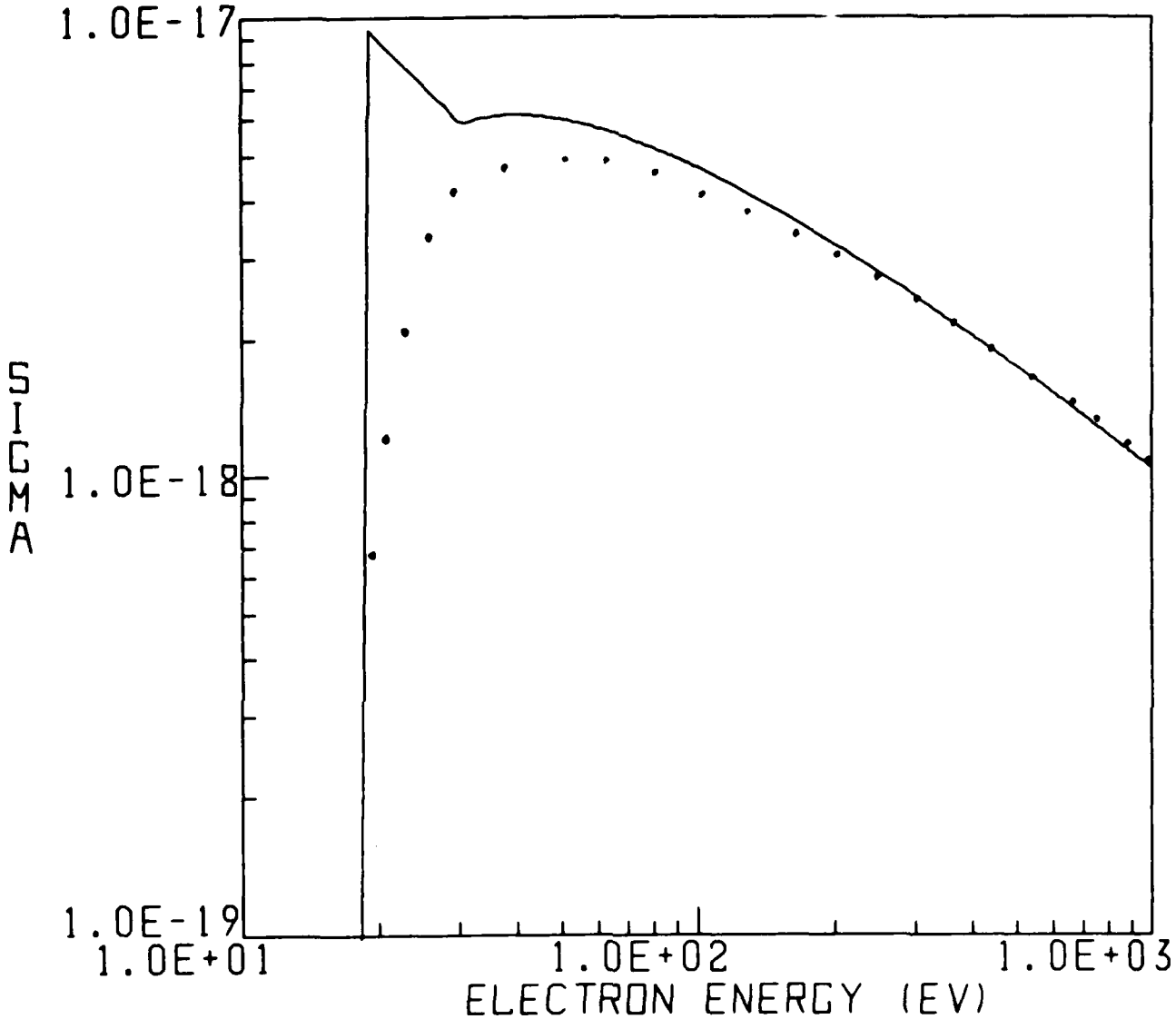

Fig. 5. Electron impact excitation cross sections for $N^+(^3P \rightarrow {}^3P^o)$ 672 Å transition (solid line - Eqs. (2) and (4), dotted line - Ref. 48).

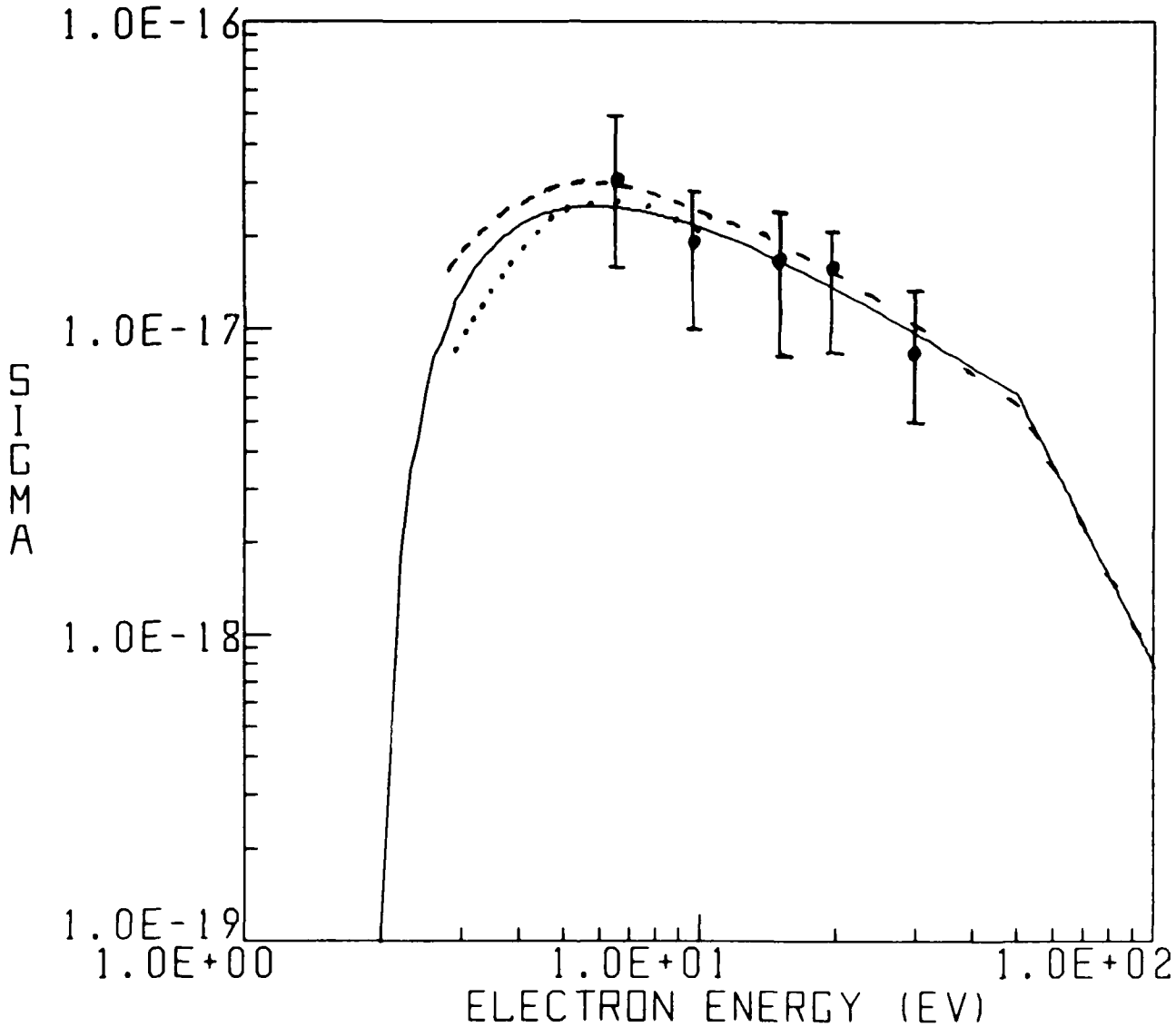

Fig. 6. Electron impact excitation cross sections for $O(^3P \rightarrow {}^1D)$ transition (solid line - Eq. (5), dotted line - Ref. 53, dashed line - Ref. 51, and circles - Ref. 50).

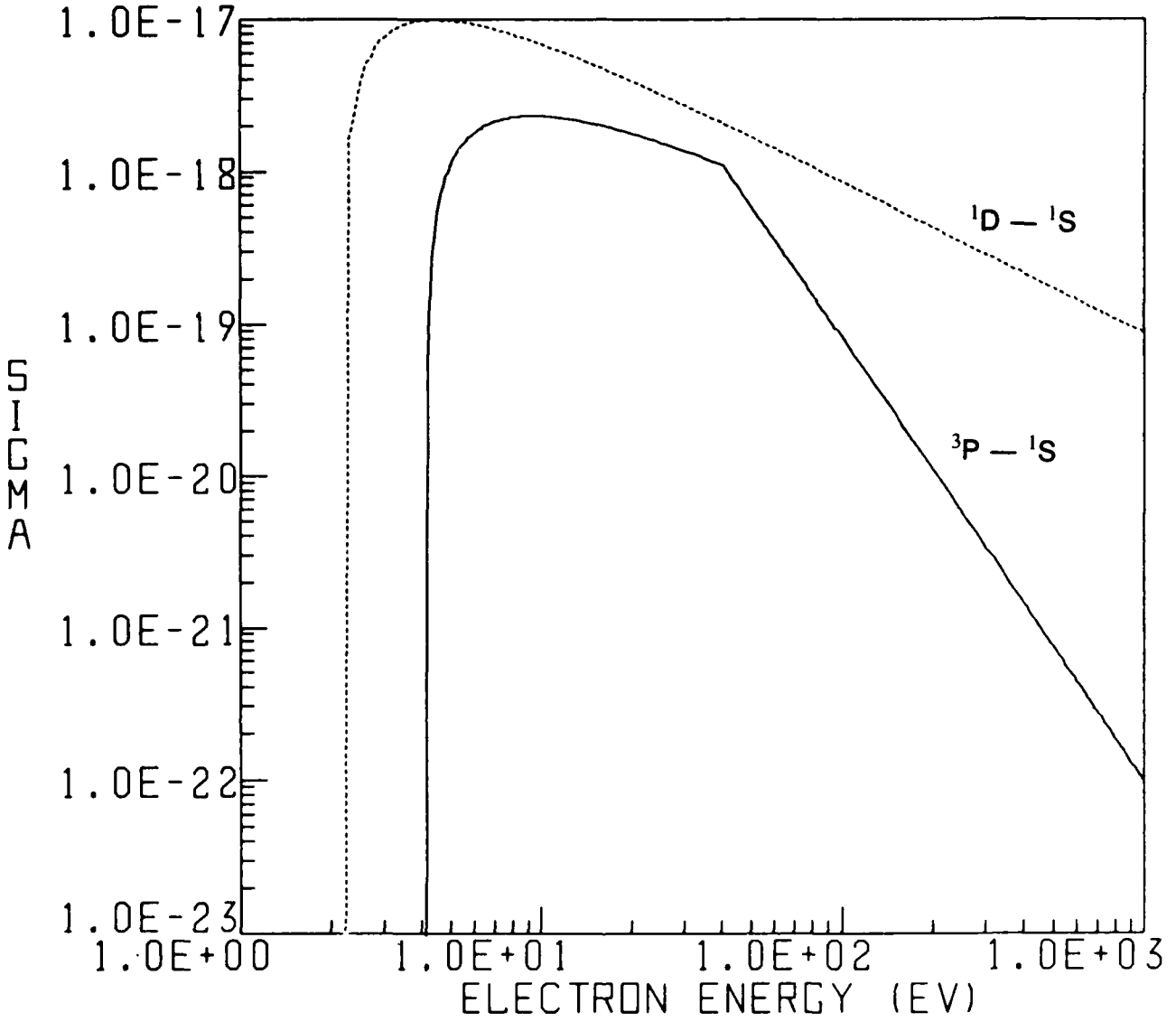

Fig. 7. Electron impact excitation cross sections for $O(^3P \rightarrow {}^1S)$ transition (solid line - Eq. (5)) and $O(^1D \rightarrow {}^1S)$ transition (dotted line - Eq. (5)).

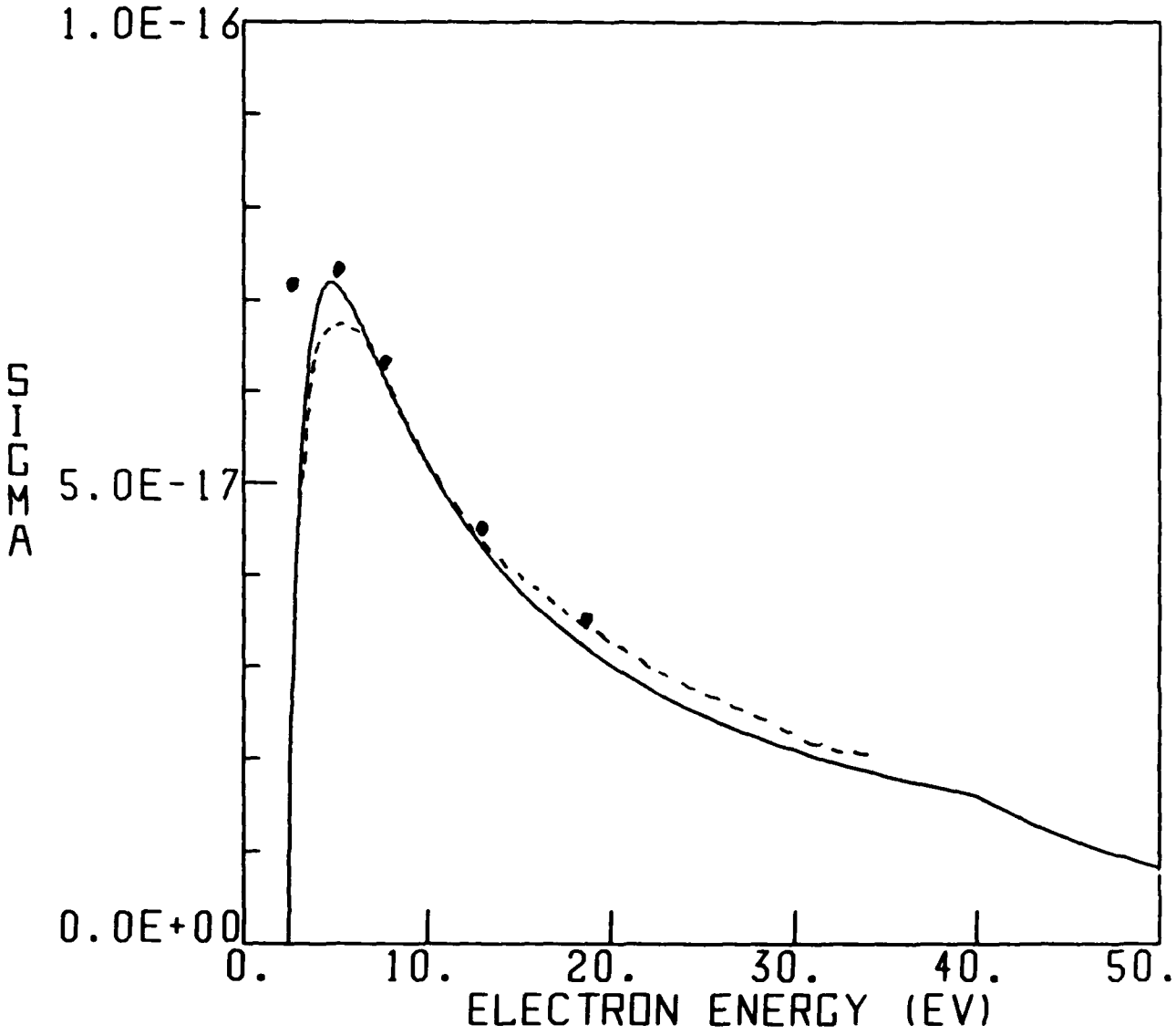

Fig. 8. Electron impact excitation cross sections for $N(^4S^o \rightarrow {}^2D^o)$ transition (solid line - Eq. (5), dashed line - Ref. 57, and circles - Ref. 56).

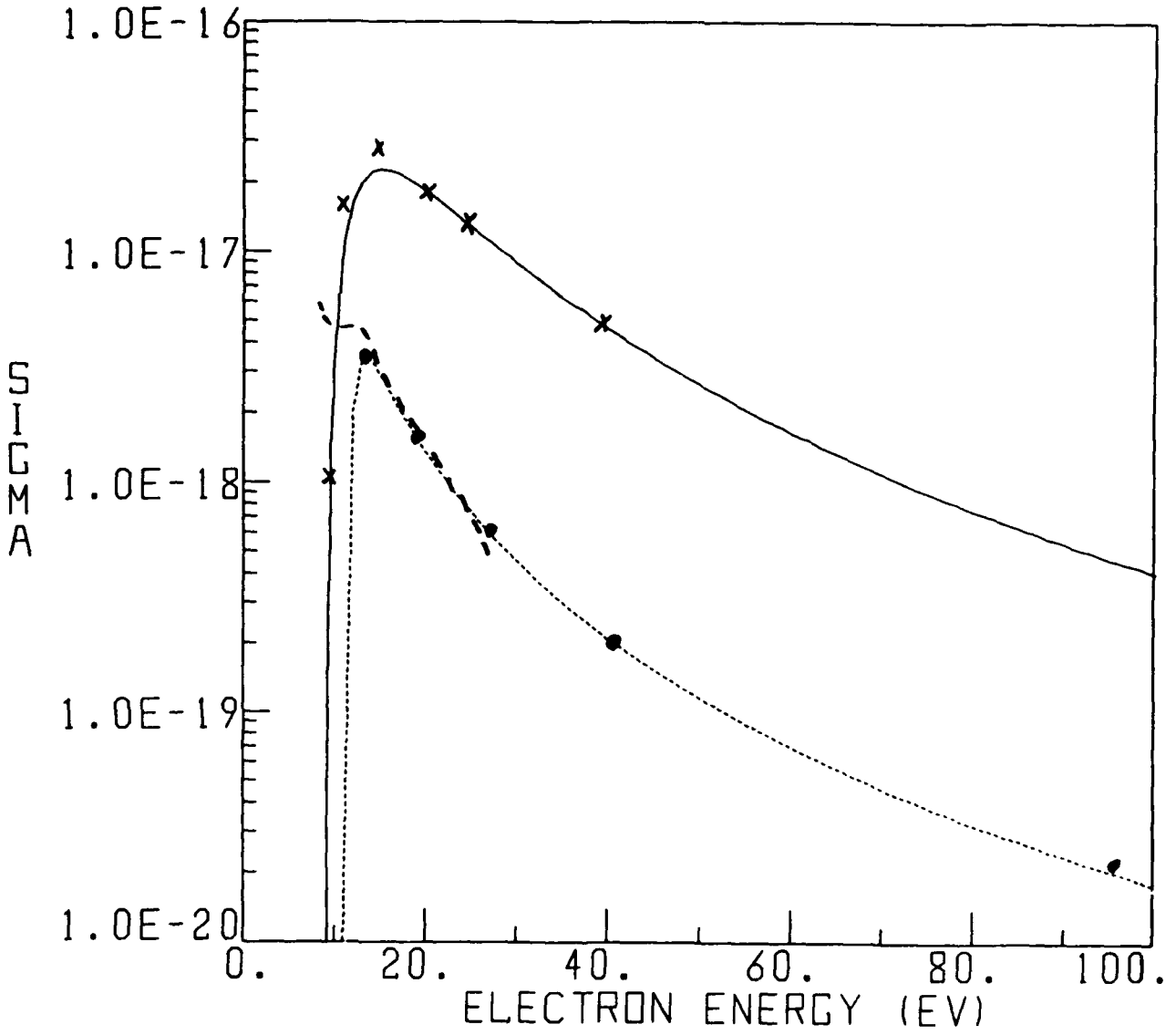

Fig. 9. Electron impact excitation cross sections for $O(^3P \rightarrow {}^5S^o)$ transition (solid line - Eq. (5), dotted line - Eq. (9), dashed line - Ref. 36, exes - Ref. 31, and circles - Ref. 37).

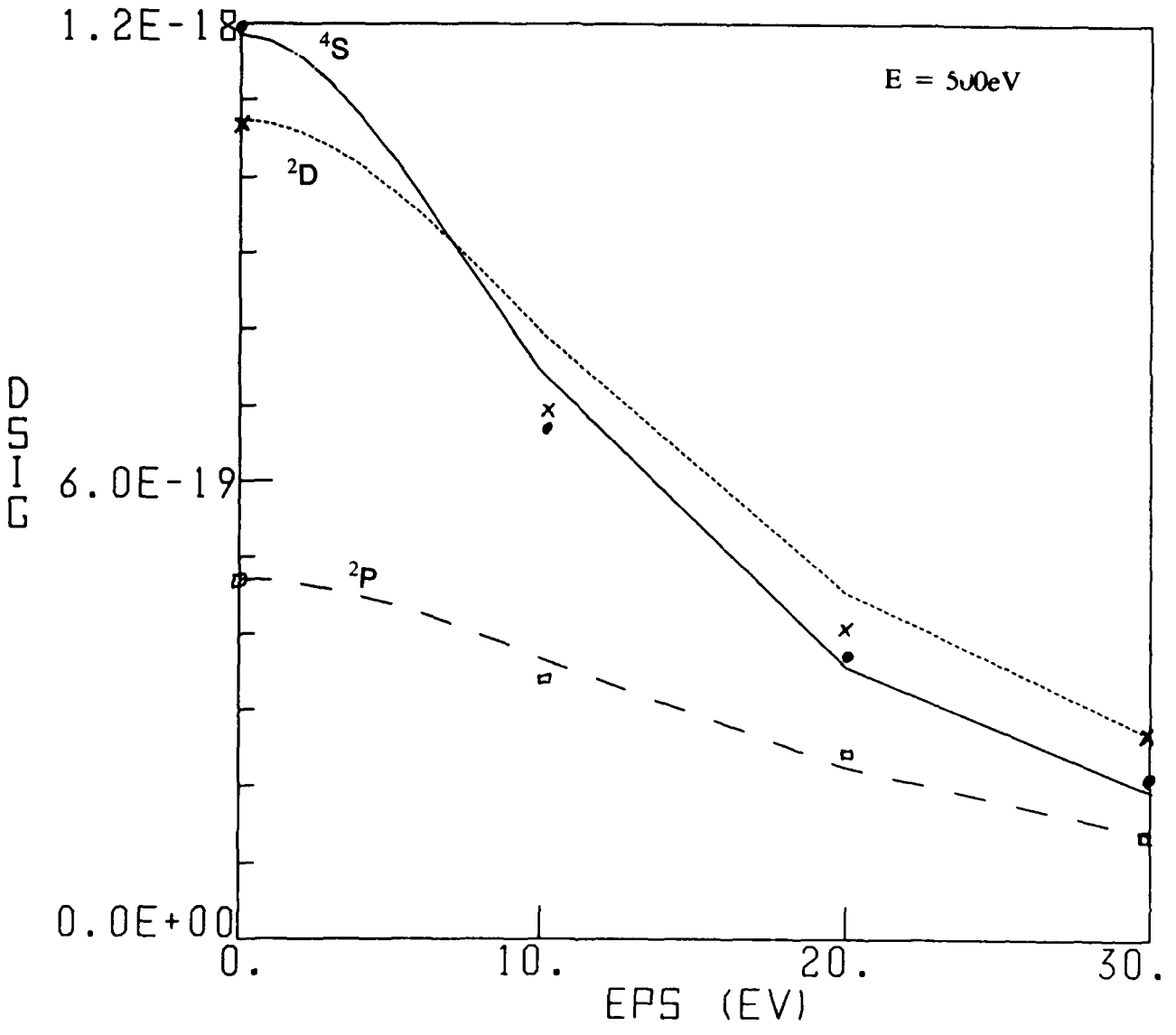

Fig. 10. Partial single differential cross sections for $O(^3P)$ ionization by a 500 eV primary electron (solid, dotted, and dashed lines - Eqs. (11 - 15); exes, circles, and squares - Ref. 66).

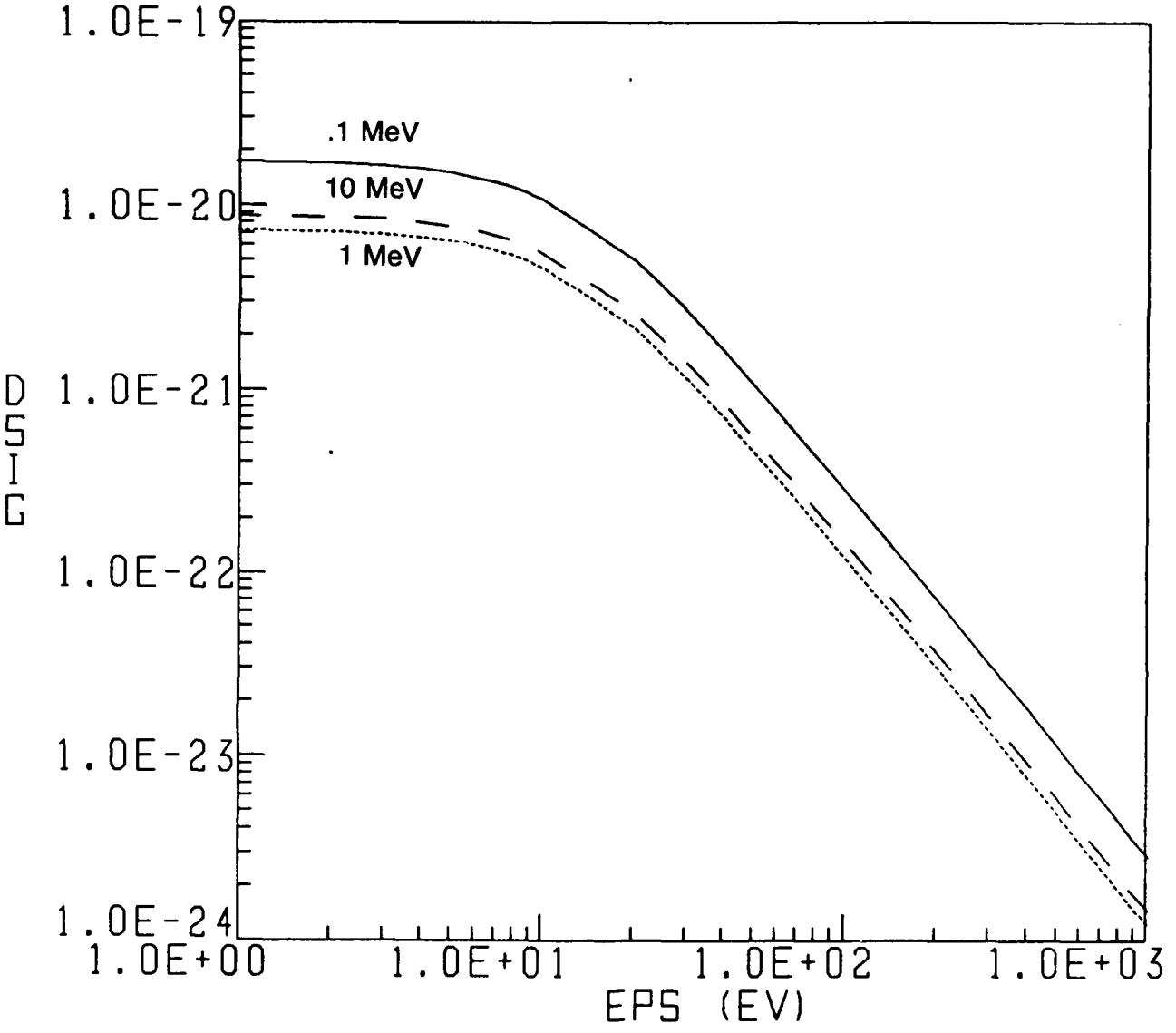

Fig. 11. Partial single differential cross sections for $O(^3P) \rightarrow O^+(^4S^o)$ for 0.1 MeV (solid line), 1.0 MeV (dotted line), and 10.0 MeV (dashed line) primaries.

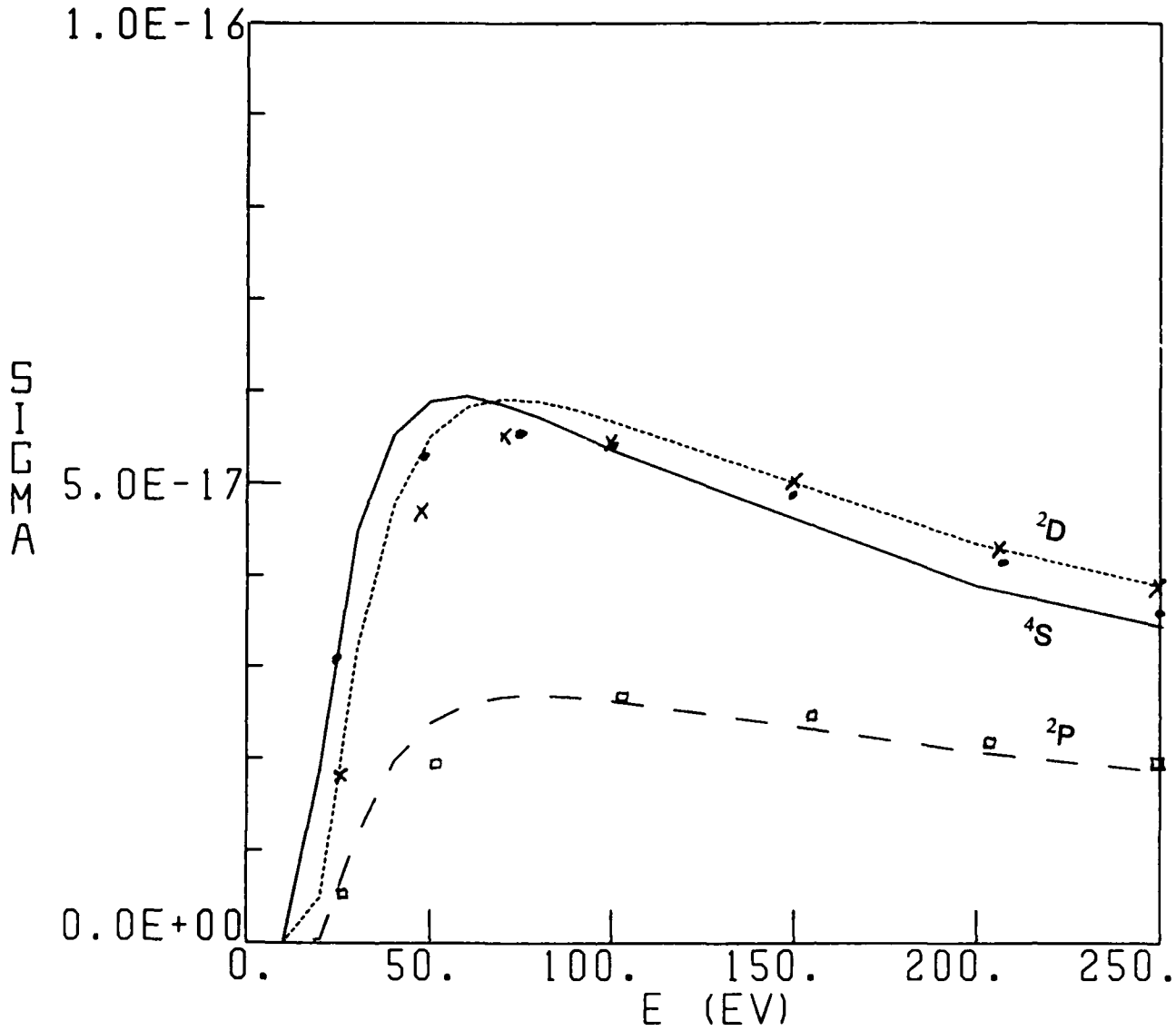

Fig. 12. Partial ionization cross sections for $O(^3P) \rightarrow O^+(^4S^o, ^2D^o, ^2P^o)$ (solid, dotted, and dashed lines - Eqs. (11 - 15), exes, circles, and squares - Ref. 66).

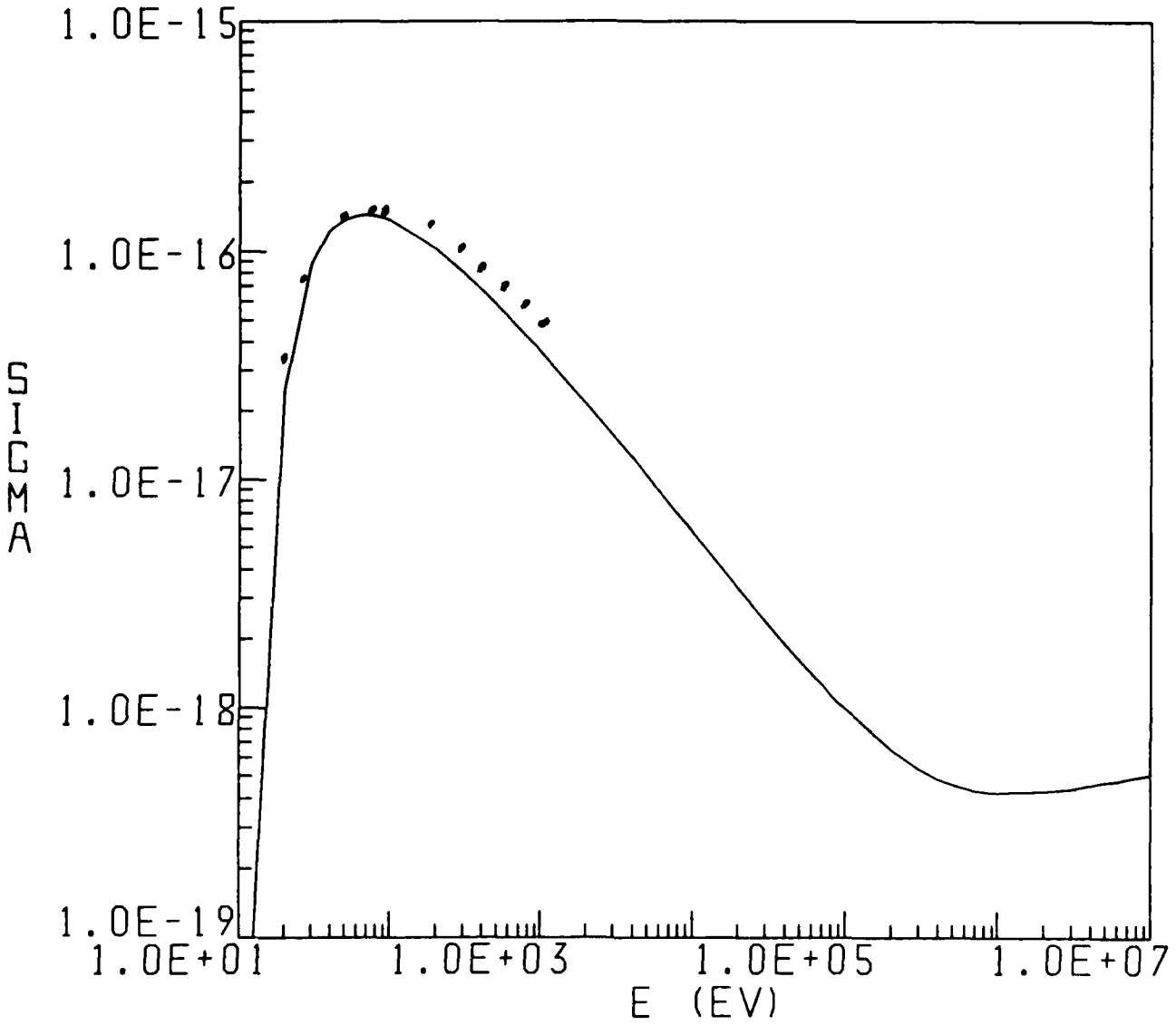

Fig. 13. Total electron impact ionization cross sections for $O(^3P)$ (solid line - Eq. (15), circles - Ref. 70).

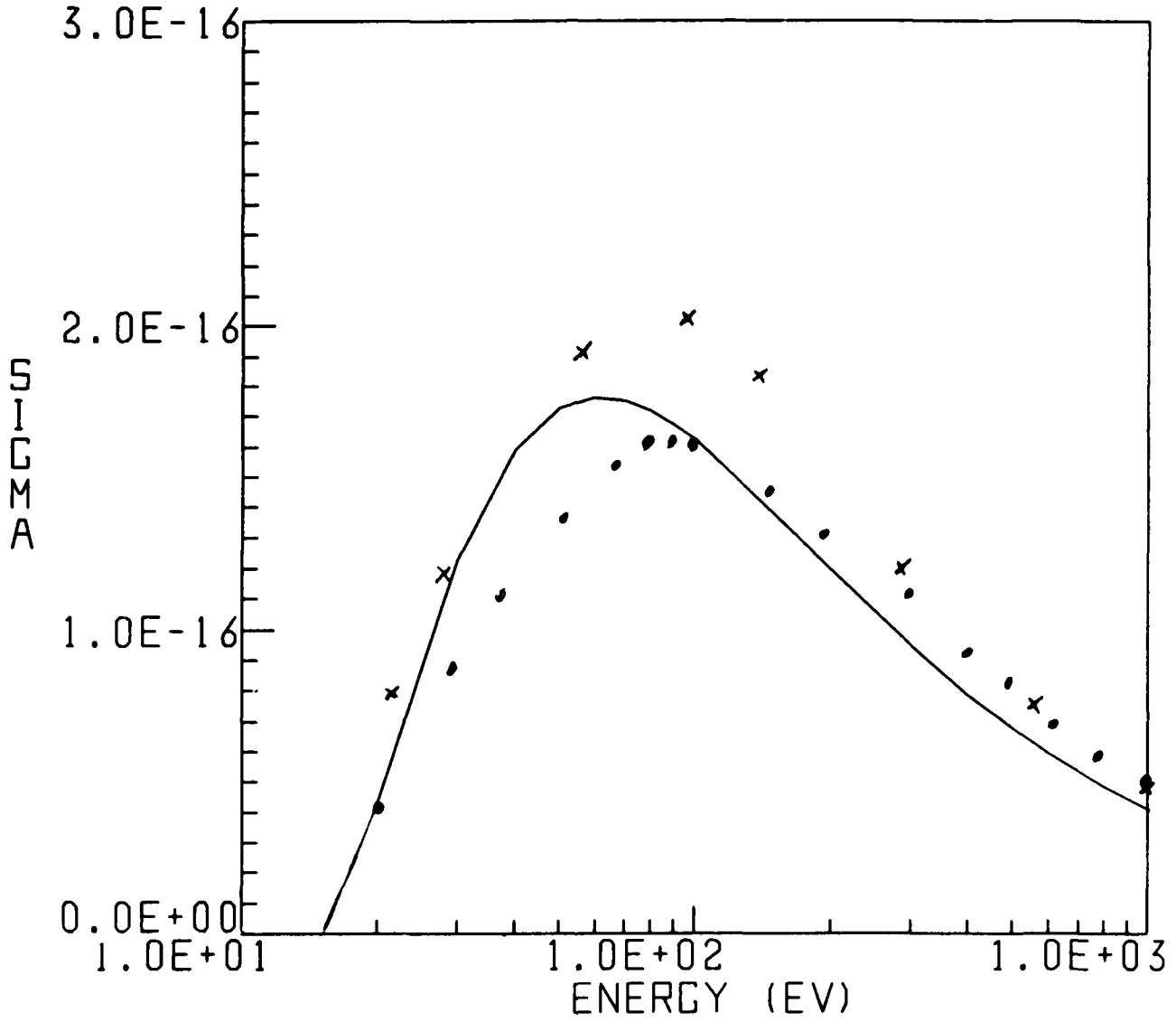

Fig. 14. Total electron impact ionization cross sections for $N(^4S^o)$ (solid line - Eq. (15), circles - Ref. 70, exes - Ref. 73).

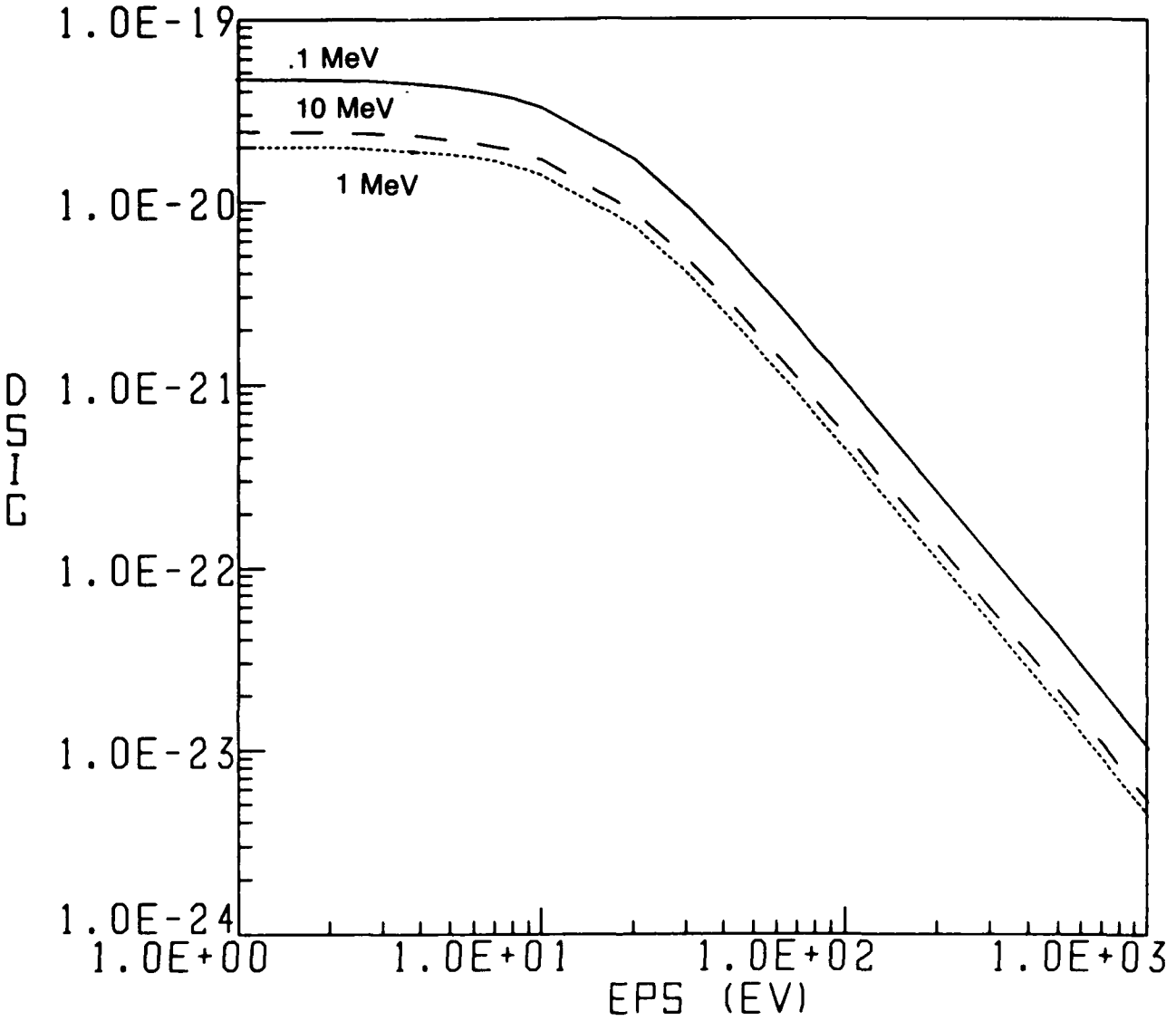

Fig. 15. Single differential cross sections for $N(^4S^o) \rightarrow N^+(^3P)$ for 0.1 MeV (solid line), 1.0 MeV (dotted line), and 10.0 MeV (dashed line) primaries.

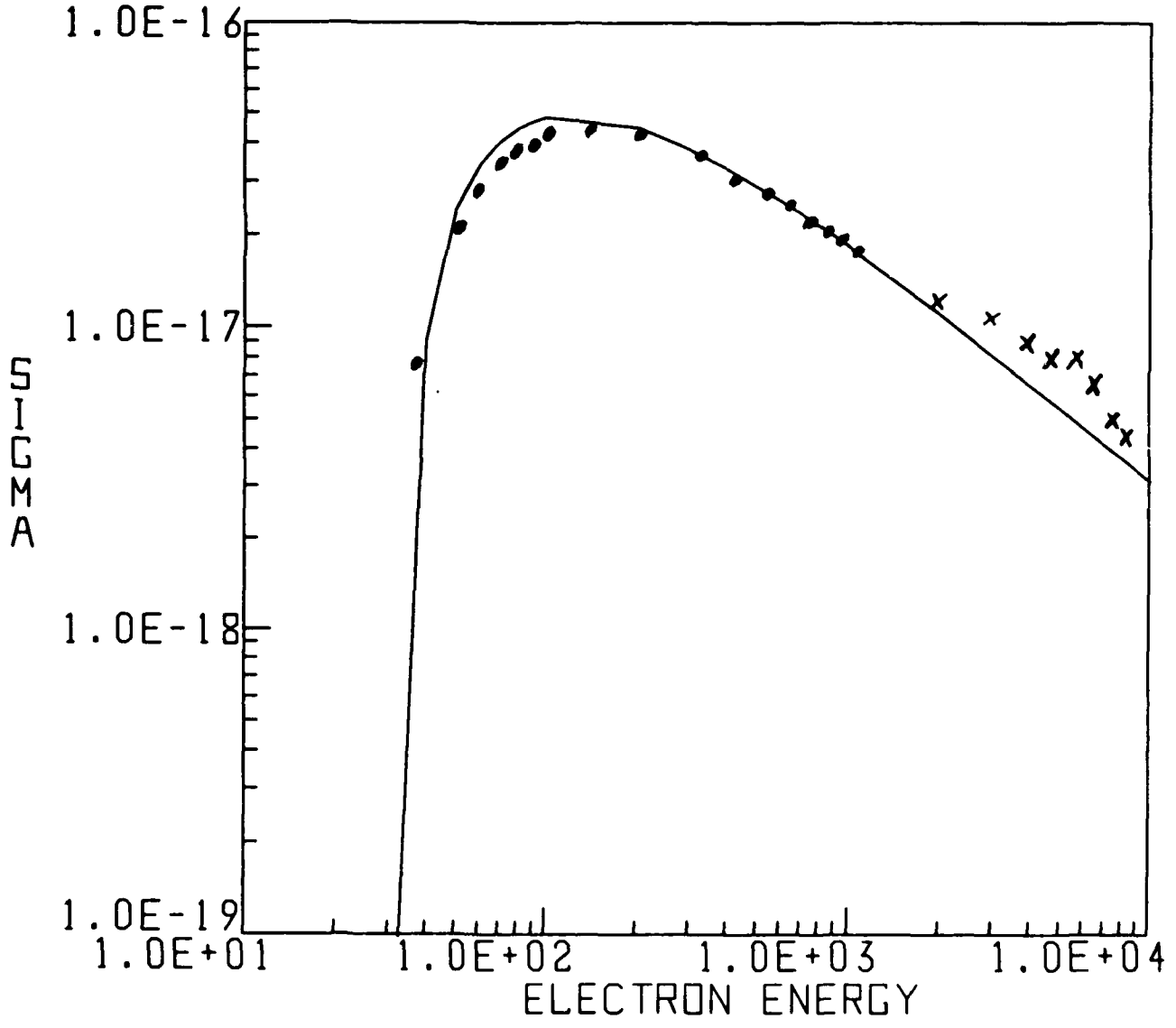

Fig. 16. Total electron impact ionization cross sections for $O^+(^4S^o)$ (solid line - Eq. (15), circles - Ref. 77, exes - Ref. 80).

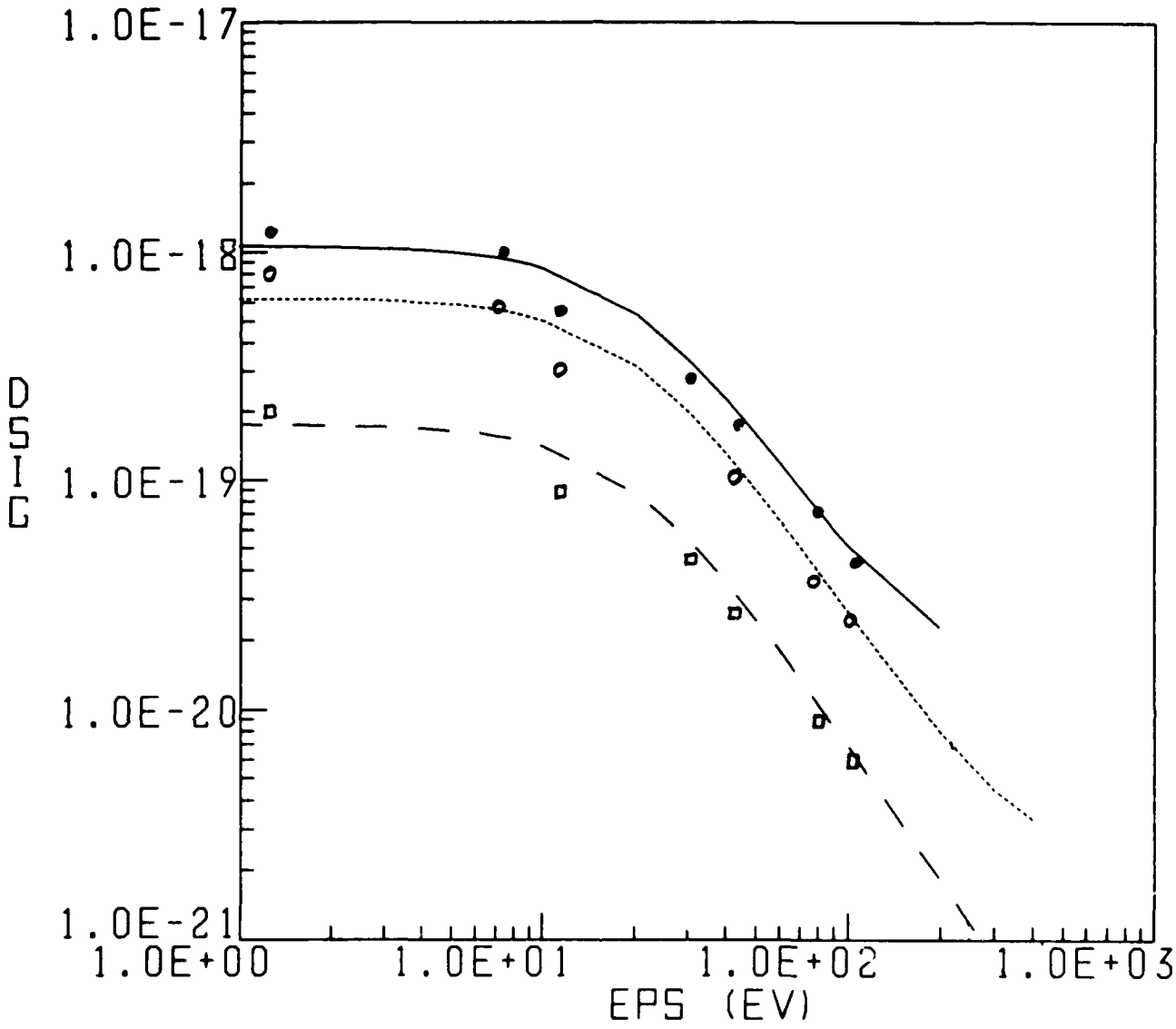

Fig. 17. Single differential cross sections for $O^+(^4S^o)$ for 500.0, 1000.0, and 5000.0 eV primaries (solid, dotted and dashed lines - Eqs. (11 - 15); solid circles, open circles, and squares - Ref. 13).

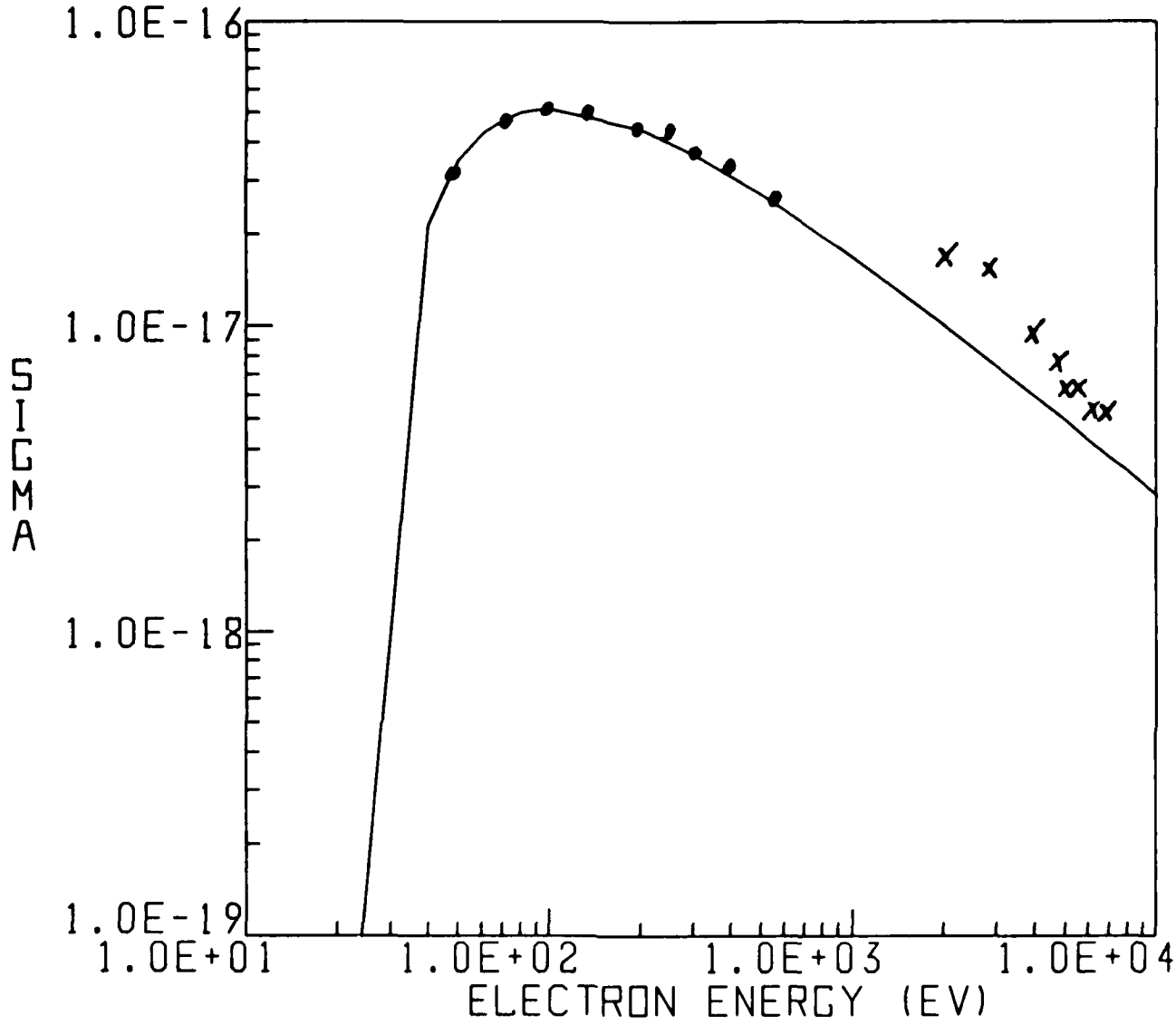

Fig. 18. Total electron impact ionization cross sections for $N^+(^3P)$ (solid line - Eq. (15), circles - Ref. 85, exes - Ref. 80).

Distribution List

Naval Research Laboratory
4555 Overlook Avenue, S.W.
Washington, D.C. 20375-5000

Attn: Dr. M. Lampe - Code 4792 (2 copies)
Dr. T. Coffey - Code 1001
Dr. J. Boris - Code 4040
Dr. M. Picone - Code 4040
Dr. J. B. Aviles - Code 4665
Dr. M. Raftel - Code 4665
Dr. S. Ossakov - Code 4700 (26 copies)
Dr. A. Ali - Code 4700.1 (30 copies)
Dr. M. Friedman - Code 4700.1
Dr. R. Taylor - BRA (4700.1) (30 copies)
Mr. I. M. Vitkovitsky - Code 4701
Dr. S. Gold - Code 4740
Dr. A. Robson - Code 4760
Dr. M. Raleigh - Code 4760
Dr. R. Meger - Code 4763
Dr. D. Murphy - Code 4763
Dr. R. Pechacek - Code 4763
Dr. G. Cooperstein - Code 4770
Dr. D. Colombant - Code 4790
Dr. R. Fernsler - Code 4790
Dr. I. Haber - Code 4790
Dr. R. F. Hubbard - Code 4790
Dr. G. Joyce - Code 4790
Dr. Y. Lau - Code 4790
Dr. S. P. Slinker - Code 4790
Dr. P. Sprangle - Code 4790
W. Brizzi - Code 4790A
Code 4790 (20 copies)
Library - Code 2628 (20 copies)
D. Wilbanks - Code 2634
Code 1220

Air Force Office of Scientific Research
Physical and Geophysical Sciences
Bolling Air Force Base
Washington, DC 20332
Attn: Major Bruce Smith

Air Force Weapons Laboratory
Kirtland Air Force Base
Albuquerque, NM 87117
Attn: W. Baker (AFWL/NTYP)
D. Dietz (AFWL/NTYP)
Lt Col J. Head

U. S. Army Ballistics Research Laboratory
Aberdeen Proving Ground, Maryland 21005
Attn: Dr. Donald Eccleshall (DRXBR-BM)
Dr. Anand Prakash

Avco Everett Research Laboratory
2385 Revere Beach Pkwy
Everett, Massachusetts 02149
Attn: Dr. R. Patrick
Dr. Dennis Reilly

Ballistic Missile Def. Ad. Tech. Ctr.
P.O. Box 1500
Huntsville, Alabama 35807
Attn: Dr. M. Havie (BMDSATC-1)

Chief of Naval Material
Office of Naval Technology
MAT-0712, Room 503
800 North Quincy Street
Arlington, VA 22217
Attn: Dr. Eli Zimet

Cornell University
369 Upson Hall
Ithaca, NY 14853
Attn: Prof. David Hammer

DASIAC - DETIR
Kaman Tempo
25600 Huntington Avenue, Suite 500
Alexandria, VA 22303
Attn: Mr. P. Wimenitz

Defense Advanced Research Projects Agency
1400 Wilson Blvd.
Arlington, VA 22209
Attn: Dr. Shen Shey
Dr. H. L. Buchanan

Department of Energy
Washington, DC 20545
Attn: Dr. Wilmot Hess (ER20:GTN,
High Energy and Nuclear
Physics)
Mr. Gerald J. Peters (G-256)

Directed Technologies, Inc.
226 Potomac School Road
McLean, VA 22101
Attn: Dr. Ira P. Kuhn
Dr. Nancy Chesser

C. S. Draper Laboratories
555 Technology Square
Cambridge, Massachusetts 02139
Attn: Dr. E. Olsson
Dr. L. Matson

Institute for Fusion Studies
University of Texas at Austin
RLM 11.218
Austin, TX 78712
Attn: Prof. Marshall N. Rosenbluth

Intelcom Rad Tech.
P.O. Box 81087
San Diego, California 92138
Attn: Dr. W. Selph

Joint Institute for Laboratory
Astrophysics
National Bureau of Standards and
University of Colorado
Boulder, CO 80309
Attn: Dr. Arthur V. Phelps

Kaman Sciences
1500 Garden of the Gods Road
Colorado Springs, CO 80933
Attn: Dr. John P. Jackson

Lavrence Berkeley Laboratory
University of California
Berkeley, CA 94720
Attn: Dr. Edward P. Lee

Lavrence Livermore National Laboratory
University of California
Livermore, California 94550
Attn: Dr. Richard J. Briggs
Dr. Simon S. Yu
Dr. Frank Chambers
Dr. James W.-K. Mark, L-477
Dr. William Favley
Dr. William Barletta
Dr. William Sharp
Dr. Daniel S. Prono
Dr. John K. Boyd
Dr. Kenneth W. Struve
Dr. John Clark
Dr. George J. Caporaso
Dr. William E. Martin
Dr. Donald Prosnitz

Lockheed Missiles and Space Co.
3251 Hanover St.
Bldg. 205, Dept 92-20
Palo Alto, CA 94304
Attn: Dr. John Siambis

Los Alamos National Scientific Laboratory
P.O. Box 1663
Los Alamos, NM 87545
Attn: Dr. L. Thode
Dr. M. A. Mostrom, MS-608
Dr. H. Dogliani, MS-5000
Dr. R. Carlson
Ms. Leah Baker, MS-P940
Dr. Carl Ekdahl

Maxwell Laboratories Inc.
8888 Balboa Avenue
San Diego, CA 92123
Attn: Dr. Ken Whitham

McDonnell Douglas Research Laboratories
Dept. 223, Bldg. 33, Level 45
Box 516
St. Louis, MO 63166
Attn: Dr. Evan Rose
Dr. Carl Leader

Mission Research Corporation
EM Systems Applications
1720 Randolph Road, S.E.
Albuquerque, NM 87106
Attn: Dr. Brendan Godfrey
Dr. Thomas Hughes
Dr. Lavrence Wright
Dr. A. B. Newberger

Mission Research Corporation
P. O. Draver 719
Santa Barbara, California 93102
Attn: Dr. C. Longmire
Dr. N. Carron

National Bureau of Standards
Gaithersburg, Maryland 20760
Attn: Dr. Mark Wilson

Naval Surface Weapons Center
White Oak Laboratory
Silver Spring, Maryland 20903-5000
Attn: Dr. R. Cavley
Dr. J. W. Forbes
Dr. B. Hui
Mr. W. M. Hinckley
Mr. N. E. Scofield
Dr. E. C. Whitman
Dr. M. H. Cha
Dr. H. S. Uhm
Dr. R. Fiorito
Dr. K. T. Nguyen
Dr. R. Stark
Dr. R. Chen

Office of Naval Research
800 North Quincy Street
Arlington, VA 22217
Attn: Dr. C. W. Roberson
Dr. M. Moss

Office of Naval Research (2 copies)
Department of the Navy
Code 01231C
Arlington, VA 22217

Office of Under Secretary of Defense
Research and Engineering
Room 3E1034
The Pentagon
Washington, DC 20301
Attn: Mr. John M. Bachkosky

ORI, Inc.
1375 Piccard Drive
Rockville, MD 20850
Attn: Dr. C. M. Huddleston

Physical Dynamics, Inc.
P.O. Box 1883
La Jolla, California 92038
Attn: Dr. K. Brueckner

Physics International, Inc.
2700 Merced Street
San Leandro, CA. 94577
Attn: Dr. E. Goldman

Princeton University
Plasma Physics Laboratory
Princeton, NJ 08540
Attn: Dr. Francis Perkins, Jr.

Pulse Sciences, Inc.
600 McCormack Street
San Leandro, CA 94577
Attn: Dr. Sidney Putnam
Dr. John Bayless

Sandia National Laboratory
Albuquerque, NM 87115
Attn: Dr. Bruce Miller
Dr. Collins Clark
Dr. Barbara Epstein
Dr. John Freeman
Dr. Charles Frost
Dr. Gordon T. Leifeste
Dr. Gerald N. Hays
Dr. James Chang
Dr. Michael G. Mazerakis
Dr. John Wagner
Dr. Ron Lipinski

Science Applications Intl. Corp.
P. O. Box 2351
La Jolla, CA 92038
Attn: Dr. Rang Tsang

Science Applications Intl. Corp.
5150 El Camino Road
Los Altos, CA 94022
Attn: Dr. R. R. Johnston
Dr. Leon Feinstein
Dr. Douglas Keeley

Science Applications Intl. Corp.
1710 Goodridge Drive
McLean, VA 22102
Attn: Mr. W. Chadsey
Dr. A Drobot
Dr. K. Papadopoulos
Dr. B. Hui

Commander
Space & Naval Warfare Systems Command
PMW-145
Washington, DC 20363-5100
Attn: CAPT J. D. Fontana
CDR W. Bassett

SRI International
PS0-15
Molecular Physics Laboratory
333 Ravensvood Avenue
Menlo Park, CA 94025
Attn: Dr. Donald Eckstrom

Strategic Defense Initiative Org.
1717 H Street, N. W.
Washington, DC 20009
Attn: Lt Col R. L. Gullickson
Dr. J. Ionson
Dr. D. Duston

Strategic Defense Initiative Office
Directed Energy Weapons Office, The
Pentagon
Office of the Secretary of Defense
Washington, DC 20301-7100
Attn: Dr. C. F. Sharn (OP0987B)

Titan Systems, Inc.
9191 Towne Centre Dr.-Suite 500
San Diego, CA 92122
Attn: Dr. R. M. Dove

University of California
Physics Department
Irvine, CA 92664
Attn: Dr. Gregory Benford

University of Maryland
Physics Department
College Park, MD 20742
Attn: Dr. Y. C. Lee
Dr. C. Grebogi

University of Michigan
Dept. of Nuclear Engineering
Ann Arbor, MI 48109
Attn: Prof. Terry Kammash
Prof. R. Gilgenbach

Director of Research
U.S. Naval Academy
Annapolis, MD 21402 (2 copies)